RECYCLED CARBON FIBER (rCF) REINFORCED POLYPROPYLENE (PP) COMPOSITES USING CARDING

A Thesis Presented for the

Master of Science

Degree

The University of Tennessee, Knoxville

Vinit Dilip Chaudhary

May 2023

Copyright © 2023 by
Vinit Dilip Chaudhary

ACKNOWLEDGEMENTS

This work would not have been possible without the support of several great individuals. I will always be thankful for the help of my family, friends, colleagues, advisors, mentors, and support staff. I sincerely want to thank my parents, Dilip Chaudhari, and Sharda Chaudhari, for their continuous love and support. In addition, I would like to express my gratitude to my aunt Savita Chaudhari for instilling in me the principles that have helped shape me into the person I am today. I would also like to thank my fiancée, Melina, for the unconditional love, support, and patience she has shown me throughout this graduate school journey.

I express my deep appreciation to my advisor, Dr. Uday Vaidya, for having faith in me and providing me with ample opportunities and continuous guidance that has helped me develop into the dedicated professional I am today. I want to offer special thanks to my committee members, Dr. Merlin Theodore and Dr. Ryan Ginder, for their time and input in my research. Also, I would like to thank Dr. Duty, Dr. Harper, and Dr. Compton for letting me use their lab space for various experiments related to my thesis work. Further, I would like to thank Jaydeep Kolape and Dr. Gerald Egeland for assisting me with SEM imaging. I am also thankful to Dwynn Nyquist from Resodyn Corporation for helpful discussions on the RAM technique.

The completion of this work would not have been possible without the help of my wonderful labmates and colleagues. To my outstanding undergraduate student, Sam Botto, thank you for all your help. I would also like to thank Tyler Sundstrom and John Klepzig for being excellent undergraduate students and for helping me with a few critical research tasks. Next, I am very thankful to Stephen Sheriff, Vanina Ghossein, and Lexi Rice for all the administrative support. I want to acknowledge and thank Dr. Pritesh Yeole, a researcher at the lab, for continuous guidance throughout my time at the lab, both as an undergraduate and graduate student. I am also thankful to all the current and former graduate students and friends, especially Surbhi Kore, Sanjita Wasti, Ryan Spencer, Benjamin Schwartz, Saurabh Pethe, Hicham Ghossein, Warren Smith, Kaustubh Mungale, Akash Phadatare, Georges Chahine, Romeo Fono-Tamo, Abdallah Ragab, and the rest of the Dr. Vaidya's group, who have helped me along the way.

Finally, this work would not have been possible without the funding support from the Department of Energy (DOE)- Institute for Advanced Composites Manufacturing Institute (IACMI), and the University of Tennessee's MABE (Mechanical Aerospace and Biomedical Engineering) department.

ABSTRACT

The use of carbon fiber (CF) composites is growing in non-aerospace markets, such as the automotive and transportation sectors. More than 30% of the CF produced ends up as waste material in landfills at end of life (EOL) from sources such as decommissioned aircraft and industrial components. CF retains its properties over decades and offers significant benefits if recycled and repurposed. Recycled CFs (rCF) are less expensive than virgin fibers, and composites made from rCF have mechanical properties that are acceptable for a variety of non-aerospace applications. In this study, a homogenous mixture of rCF-polypropylene (PP) was achieved using the Resonant Acoustic Mixing (RAM) technique, where water was used as a mixing solvent. The nonwoven composite's mechanical properties and molding conditions are influenced by how well the fibers are aligned. Randomly oriented nonwovens have similar mechanical properties in all directions and can be manufactured using a wet-laid (WL) process, whereas highly aligned nonwoven textiles can be manufactured using carding process. Therefore, nonwoven rCF-PP mats were fabricated using carding and WL techniques to understand the effect of fiber orientation on mechanical properties. In this study we observed that carding machine parameters such as pin length, cylinder width, distance between cylinders have influence on final mechanical properties. The mats were compression molded to obtain consolidated panels. Mechanical, microscopic, and fiber length distribution characterization was performed to determine the properties variation between the two manufacturing techniques. The flexural strength and modulus of carding in the machine (along the fibers) direction (MD) was 22% (from 86.89 ± 5.1 MPa to 105.99 ± 12.42 MPa) and 72% (from 5.14 ± 0.5 GPa to 8.85 ± 1.3 GPa), respectively higher as compared to wet-laid. Further, the tensile strength and modulus of carded composites in MD were 75% (from 35.51 ± 5.1 MPa to 62.10 ± 4.8 MPa) and 110.8% (from 6.58 ± 1.81 GPa to 13.87 ± 1.57 GPa), respectively higher than WL process. This work has broad applications in product development with rCF in many commercial and commodity sectors such as sporting goods, automotive, medical devices, etc.

Keywords: Recycled carbon fiber, carding, wet-laid, Resonant Acoustic Mixing (RAM), fiber length distribution.

TABLE OF CONTENTS

CHAPTER 1- INTRODUCTION 1

CHAPTER 2- LITERATURE REVIEW 3

2.1 - CARBON FIBER REINFORCED POLYMERS 3
2.2 - RECYCLED CARBON FIBERS 4
2.2.1 RECYCLING PROCESSES 6
2.3 – FIBERS MIXING TECHNIQUES 8
2.4 –TEXTILE NONWOVENS USING RECYCLED CARBON FIBERS 13
2.4.1 ISOTROPIC NONWOVEN COMPOSITES 16
2.4.1.1. AIR-LAID 16
2.4.1.2 WET-LAID 18
2.4.2 ANISOTROPIC NONWOVEN COMPOSITES 21
2.4.2.1 CARDING 21

CHAPTER 3- MATERIALS AND METHODS 28

3.1 MATERIALS 28
3.2 FIBERS MIXING TECHNIQUE 28
3.3 ANISOTROPIC NONWOVENS MANUFACTURING VIA CARDING PROCESS 28
3.4 ISOTROPIC NONWOVENS MANUFACTURING VIA WET-LAID PROCESS 37
3.5 COMPRESSION MOLDING 37
3.6 FIBER LENGTH DISTRIBUTION (FLD) 39
3.7 MECHANICAL CHARACTERIZATION 42
3.8 SCANNING ELECTRON MICROSCOPY (SEM) 43
3.9 DIFFERENTIAL SCANNING CALORIMETRY (DSC) 43
3.10 THERMOGRAVIMETRIC ANALYSIS (TGA) 43

CHAPTER 4- RESULTS AND DISCUSSIONS 44

4.1 FIBER LENGTH DISTRIBUTION 44
4.2 FIBERS MIXING TECHNIQUE 47
4.3 MECHANICAL CHARACTERIZATION 47
4.4 THERMAL ANALYSIS 61
4.5 THEORETICAL APPROACH 65

CHAPTER 5- CONCLUSIONS 71

REFERENCES 73

VITA 85

LIST OF TABLES

Table 3.1: rCF and PP material specifications 30
Table 3.2: rCF-PP fibers mixing outline 30
Table 3.3: rCF-PP mixing with different parameters using LabRAM II 31
Table 3.4: Carver press parameters for rCF-PP 40
Table 4.1: Results of premixing of rCF-PP using RAM technique 48
Table 4.2: Characteristics of composite components 48
Table 4.3:Mechanical properties of carder-2, WL and neat PP samples. 54
Table 4.4: Comparison of theoretical and experimental results of tensile modulus of carded MD and WL composites. 70

LIST OF FIGURES

Figure 1: Global demand for carbon fiber [25] and estimated waste carbon fiber [26] 5
Figure 2: Closed loop recycling of carbon fiber composite- The CFRP components of a decommissioned aircraft, such as a Boeing 747, has around 30-40,000 lbs. of carbon fiber composites. The carbon fiber in these components is reclaimed via pyrolysis and similar processes. Carbon fiber is transformed into intermediary forms appropriate for composite manufacturing. The recycled carbon intermediate is then converted into a final composite part using resin transfer molding (RTM) or other processes. A final composite part is then installed on a vehicle- in this scenario a corvette part for under the hood [42], [43]. 9
Figure 3: (a) V-Shaped tumbler mixer [48], (b) Fluidized-bed mixer [48], (c) High shear mixer [41], (d) Hopper mixer [48], and (e) Single-screw extruder [41]..... 14
Figure 4: RAM mixing mechanism illustrating formation of micro mixing zones during the mixing process 15
Figure 5: (a) A bench top LabRAM II resonant acoustic mixer with max payload of 2.2 pounds (Source: Resodyn Acoustic Mixers, Inc. [53]), (b) RAM5 mixer for production scale batch mixing capable of mixing 80 pounds of material at a time (Source: Resodyn Acoustic Mixers, Inc. [54]) 15
Figure 6: The WL process (adapted from [12]); (a) Fiber dispersion in water through mechanical mixing, (b) water drainage and nonwoven fiber web formation on conveyor belt, (c) consolidation of nonwoven fiber web into roll using take up system after drying..... 19
Figure 7: Air-laid process (adapted from [11]); Fiber mixture is fed using feed rollers where licker-in cylinder takes up the fibers. High velocity airflow removes the fibers from licker-in which forms a nonwoven fiber web on permeable screen on conveyor belt..... 19
Figure 8: Carding process schematic (adapted from [7]); The fiber mixture is fed via feed rollers where taker-in takes up the fibers and transfers onto the main cylinder. In carding zone, the worker and stripper work simultaneously with main cylinder for

stripping and blending of fibers. In doffer transfer zone, the fibers are stripped off from main cylinder via doffer cylinder resulting in a nonwoven carded preform in web formation zone..... 23
Figure 9: As received rCF from ELG Carbon fiber Ltd. (Mean fiber length ~ 5mm)..... 30
Figure 10: Before mix 4: rCF and PP fibers in water before RAM..... 31
Figure 11: After mix 4: Homogeneous rCF-PP fiber mixture after RAM..... 31
Figure 12: Manual standard drum carder (carder 1) with two cylinders. Main cylinder (width 9.5 in., diameter 7 in., pin length 0.5 in., and 72 TPI (teeth per inch) 33
Figure 13: Manual deluxe baby drum carder (carder 2) with two cylinders. Main cylinder (width 4 in., diameter 7 in., pin length 0.625 in., and 72 TPI (teeth per inch))..... 33
Figure 14: Manufacturing rCF-PP nonwoven mat using carder 1; (a) Both drums covered with peel ply fabric, (b) rCF-PP fiber mixture fed to licker-in cylinder, (c,d,e) carder drums covered with fibers after continuous carding, and (f) removal of nonwoven rCF-PP carded mat with supporting peel ply fabric..... 35
Figure 15: Manufacturing rCF-PP nonwoven mats using carder 2; (a) rCF-PP fibers fed to licker-in cylinder, (b,c) carder drums covered with fibers after continuous carding, (d) rCF bundles collected on fiber catching tray during carding, (e) nonwoven rCF-PP carded mats..... 36
Figure 16: Lab scale WL mixer..... 38
Figure 17: Isotropic rCF-PP nonwoven WL mat (12 in. x 12 in.)..... 38
Figure 18: Compression molded rCF-PP panels. (a) Unidirectional carded panel (30% fiber weight fraction, panel thickness: 2.9 mm), (b) Isotropic WL panel (30% fiber weight fraction, panel thickness: 2.8 mm)..... 40
Figure 19: (a) rCF-PP mat before burn-off; (b) rCFs after burn off, and (c) Optical image of rCFs under microscope after separating the fibers from bundles via ultrasonic method..... 41
Figure 20: Carder 1- FLD study using both tweezer and ultrasonic method..... 46
Figure 21: Carder 2- FLD study using ultrasonic method..... 46
Figure 22: Flexural strength and modulus of rCF-PP composite showing standard deviation manufactured via carder 1 using mix 1-5..... 50

Figure 23: Flexural strength and modulus of rCF-PP carded, and WL composite manufactured via carder 1 with only water as mixing solvent in RAM 50
Figure 24: Tensile strength and modulus of rCF-PP carded, and WL composite manufactured via carder 1 51
Figure 25: ILSS strength of rCF-PP carded, and WL composite manufactured via carder 1 51
Figure 26: Flexural strength and modulus of rCF-PP carded, and WL composite manufactured using carder 2 55
Figure 27: Load vs. displacement curves of carding MD, carding 0/90, wet-laid, and neat PP 55
Figure 28: Illustration of force transfer in (a) Aligned composite and (b) Randomly oriented composite 57
Figure 29: Tensile strength and modulus of rCF-PP carded, and WL composite manufactured using carder 2 57
Figure 30: SEM image of carded MD composite tensile test specimen showing fiber alignment 58
Figure 31: SEM image of WL composite tensile test specimen showing random fiber orientation. 58
Figure 32: SEM image of carded MD composite tensile test specimen showing fiber pullout 59
Figure 33: SEM image of WL composite tensile test specimen showing poor fiber/matrix adhesion 59
Figure 34: ILSS strength of rCF-PP carded, and WL composite manufactured using carder 2 62
Figure 35: (a) Carded MD ILSS test specimen, (b) WL ILSS test specimen 62
Figure 36: Izod impact break strength of carded and WL rCF-PP composite for notched samples 63
Figure 37: Carded fractured Izod samples 64
Figure 38: WL fractured Izod samples 64
Figure 39: TGA results for neat PP and rCF-PP composite 66

Figure 40: DSC analysis for rCF-PP composite showing heat-cool-heat cycle from room temperature to 220 °C 66
Figure 41: DSC analysis for neat PP showing heat-cool-heat cycle from room temperature to 220 °C 67

CHAPTER 1- INTRODUCTION

The use of carbon fiber reinforced plastics (CFRPs) is rapidly growing in several industries such as aerospace, marine, automotive, and sports due to their outstanding mechanical properties. CFRPs have slowly replaced metals such as steel or aluminum in some areas due to the advantages of their high strength-to-weight ratio, lightweight, and durability [1]. Carbon fibers (CFs) are used in composites as reinforcement fibers which are defined by factors such as aspect ratio (length to diameter), orientation, fiber-matrix bonding, and processing conditions [2], [3]. CF composites can be either reinforced with thermoplastics or thermosets based on the application. This work will focus on carbon fiber-reinforced thermoplastics (CFRTPs) due to their high toughness, strength, and stiffness.

Furthermore, CFRTPs composites are in demand today due to their excellent recyclability. Precisely, polypropylene (PP) has caught attention because of resistant to water, lightweight, and cost-effective [1]. However, the CF composites being expensive, the applications are limited to mainly aerospace industries and haven't been mainly adopted into mass manufacturing industries such as automotive. Therefore, recycled carbon fibers (rCF) have recently emerged as a cost-effective and environment-friendly alternative to virgin carbon fibers (vCF) in several areas with excellent mechanical properties [4]. The expected annual global demand for vCF is 1.23 million tons if manufactured at $11/ kilogram (kg). However, current costs are estimated to be between $33 and $66/ kg, depending on fiber grade, which makes it extremely challenging to use CFRPs for low-cost light weighting [5], [6]. The price of rCFs may be as low as $5/ kg, which significantly improves the economic viability of carbon fiber composites for automobiles [5].

The production of vCF is a very energy-intensive process that requires 50-150 kWh/kg [7]. Such a process with a high cost of precursor material results in a high price of CF. On the contrary, the rCF can be recovered from end-of-life (EoL) composites at an energy cost as low as 3-9 kWh/kg. Therefore, rCF can be a good alternative which can be produced at a fraction of the cost while preserving nearly all the mechanical properties of

vCF [4]. However, recycling CF composites is insufficient to close the CFRP lifecycle loop. Instead, CFs reclaimed from EoL parts should be reprocessed for use in composite applications. Therefore, the next step should be to reuse rCF for specific applications [7].

After the rCF has been successfully reclaimed, it usually needs to be further processed into nonwoven intermediates before it can be used again in the composites industry. Nonwoven preforms have a significant economic value owing to their high manufacturing output and remarkable flexibility in terms of attributes such as areal density, uniform distribution, and degree of compaction [8]. Over the years several rCFRP (recycled carbon fiber reinforced plastics) remanufacturing techniques have been established. The techniques used to make textile preforms cause nonwoven composites to have varying degrees of anisotropy. This means that the nonwovens are either aligned to some degree or oriented randomly. Although randomly oriented nonwoven composites offer reduced remanufacturing costs, they also have lower achievable volume fractions and mechanical qualities [4]. On the other hand, the mechanical characteristics of the nonwoven composites and the molding conditions are both affected by the degree to which the fibers are aligned.

The production of nonwoven preforms may be accomplished using one of three commonly used and frequently used processes. Randomly oriented nonwovens, also known as isotropic nonwovens, have similar mechanical properties in all orientations, and can be manufactured using either the air-laid or the Wet-laid (WL) technique [9], [10]. Air-laid is a dry laying method in which fibers are dispersed uniformly in an airstream and then directed toward a permeable screen or conveyor, where they are deposited randomly to form of a web [11]. The WL process is very much like the papermaking process, in which fibers and water are combined to generate a fiber-water mixture. The mixture is then transferred to a head box where a continuous isotropic nonwoven web is formed [12]. Alternatively, anisotropic or aligned nonwoven textiles can be manufactured using carding process. Carding is one of the most efficient methods of orienting fibers to produce anisotropic composite material. This method mechanically separates individual fibers from the mixture and combines them to create a continuous nonwoven mat [7], [10], [11].

CHAPTER 2- LITERATURE REVIEW

2.1 – CARBON FIBER REINFORCED POLYMERS

In 1950s CFs were introduced as a result of advancements in aerospace technology. Beyond the aerospace industry, today, thermoplastic CFRPs are rapidly making their way into the automotive and sports industries due to their high mechanical properties, high specific strength, high toughness, and unlimited shelf-life [7], [13], [14]. However, CF composites have been slow to gain adoption in the automotive materials market due to their high cost and long cycle time. To increase the use of CFRP in the automotive industry, it will be necessary to develop cost-effective manufacturing processes and address the concerns about recyclability at the same time [15].

By 2025, the Corporate Average Fuel Economy (CAFE) instructs fuel efficiency of 50 mpg, and with Europe's vehicle emissions regulations becoming more stringent, automakers generally view the vehicle light-weighting as one significant means to stay in conformity [16]. Because of its ability to achieve the greatest levels of performance while being lightweight, composites have found widespread usage in the sport vehicle segment of the automotive sector. The recent advancements in mobility have cleared the path for autonomous guidance technologies and electric propulsion systems. These vehicles need lightweight in order to travel longer distances between recharging (electric vehicles), which has led to a new push for large volume manufacturing technologies of composites and their EoL disposal regulation [17]. Therefore, the integration of CFRPs can significantly reduce the weight of a vehicle, which can increase fuel economy. For instance, a 10% decrease in vehicle weight corresponds to a 6% decrease in fuel usage [18]. For example, the steel roof panel on the BMW M6 model was replaced with a 5.5 kg lighter CF composite, which reduced the vehicle's mass, lowered its center of gravity, and improved its stability [19]. The environmental effects of CFRP produced from vCF are very well recognized, and the scrap generated during production, EoL, and cut-off from finished parts can be recycled to create new materials such as yarns and nonwovens [20].

2.2 – RECYCLED CARBON FIBERS

The Global demand for CFRP and CF in 2017 was roughly 70.5 ktons and 114.7 ktons, respectively, bringing in revenues of about $2.59 and $14.73 billion USD, respectively [21]. In 2020 the annual global CF in the automotive industry were valued at $3.80 billion, and it was expected to increase to $6.02 billion by 2027. The overall CFRP market has shown continuous growth year after year. The expensive cost of producing vCF, in contrast to ordinary steel and aluminum, has, however, curtailed the net advantages of light weighting. The global demand for vCF was estimated to be around 1.23 million tonnes if it was produced at $11/kg; however current costs are estimated to be in the range of $33-66 per kilogram based on fiber grade, making the use of CFRPs for low-cost light weighting exceedingly challenging [6], [22] [23].

The cost of rCF can be as low as $5/kg, greatly enhancing the commercial feasibility of automobile CF composites [6]. Furthermore, the composites sector produces more waste carbon as a result of the increased demands for CFRP. According to the literature, the composite industries in both the USA and the UK produce about 3 ktons of waste carbon fiber annually [21]. Industries like aerospace, defense, automotive, and wind energy are anticipated to produce significant amounts of waste in the category of EoL components within the next two decades [21]. By 2030, between 6000 to 8000 aircraft are expected to reach the end of their useful life, generating approximately 3000 tonnes of CFRP scrap per year. Aircraft manufacturers like Boeing are planning to recycle 90% of the constituent materials. The automotive industry is also facing tougher recycling targets as average lifespan of a car is around 10-15 years. According to EU legislation, at least 85% of EoL cars must be recycled as of 2015 [24]. Figure 1 demonstrates the global demand for CFs and the estimated CF waste from the composite sector and EoL parts [25], [26].

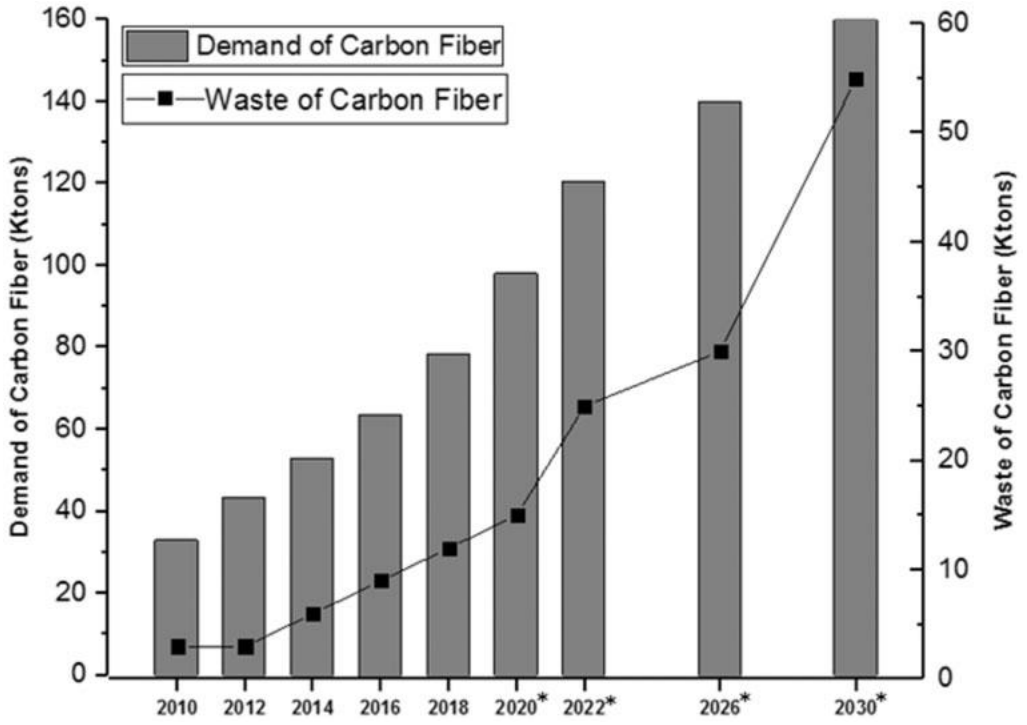


Figure 1: Global demand for carbon fiber [25] and estimated waste carbon fiber [26]

Depending on the origin the waste composite materials can be divided into three different types: Dry fiber waste, e.g., cut-offs from fabric, end of fiber roll (type-1), waste from prepregs or pre-impregnated fibers from residues (type-2), and faulty or discarded CFRP components (type-3). Type-1 waste fibers can be transformed into short, chopped fibers (~80 mm) or milled fibers (~3 mm) for integrating into textile preforms with minimal recycling efforts. For instance, fibers might need to be cut to a specific length depending on the application, but aside from that, they don't need further recycling. On the other hand, the type-2, and type-3 fibers typically need to be removed from the matrix(resin) material. The process of fiber and matrix separation is termed as recycling, since the waste material must go through numerous steps before remanufacturing [5], [27].

2.2.1 RECYCLING PROCESSES

The CFRP recycling process can broadly be categorized into three processes: mechanical, chemical, and thermal recycling. The mechanical recycling for the most part results in milled fibers or small granulates which are used as reinforcement and filler material. On the contrary, the chemical and thermal recycling process are employed in fiber reclamation technology [5].

Mechanical Recycling: In mechanical recycling, the CFRP composites are downsized by means of crushing, milling, or shredding. The resulting mixture is further divided into fibrous fragments and powdered CFRP. In mechanical recycling, the mechanical properties of the recovered fibers are significantly lowered because the length of the fibers is greatly reduced. Even after recycling, there is still some residual matrix material left behind in the product's final form to some degree. The matrix can be further partially removed using an additional process called sieving, but the final recycled fibers can only be used in injection molding or as a reinforcement material for low-value applications [27].

Thermal Recycling: To recover long discontinuous fiber from CFRP waste, thermal recycling offers an alternative recycling method that uses high temperatures to separate the matrix and reclaim the fibers. This can be achieved by two techniques as (a) fluidized bed and (b) pyrolysis [28]. (a) Fluidized bed is a very common method of recycling CFRP,

which was developed by Pickering et al [29] at the University of Nottingham. In this process, the CFRP scrap is typically shredded to 6-20mm before it enters the fluidized bed reactor The shredded material is then fed into a bed of silica sand which uses a hot air to separate the matrix and fibers at a temperature between 450 and 550 °C, under a pressure of 10 to 25 kPa. Then the loose CFs are separated from resin using a cyclone separator where the resin is completely oxidized. Typically, through this process the reclaimed rCF length falls in the range of 5-10 mm, preserving 10-75% of the tensile strength of vCF [30], [31]. This method's drawback is that the recovered CF is in the form of tangled bundles, making it very challenging to align the fibers [27], [28], [32].

(b) Pyrolysis is another most common thermal decomposition method of reclaiming CFs. Unlike the fluidized bed method, here the CFRP waste is subjected to high heat (450 °C to 700 °C) in either air or an inert atmosphere to completely burn off the matrix [27]. When the matrix is burned in the presence of air, the immense heat generated can be captured for further processing or energy production. Whereas in the inert atmosphere the chemical byproducts of the deteriorated matrix can be recovered and utilized as a synthetic gas for future power generation [5]. CFs have a strong tendency to oxidize beyond 600 °C, which has a substantial impact on their mechanical properties. Furthermore, the sizing on the fiber surface is removed, which normally has a detrimental impact on the fiber [33]. ELG Carbon Fiber Ltd (UK) which was recently acquired by Gen 2 Carbon (UK) is one of the notable CF recycling companies in the market. The company claims that pyrolyzed rCF is 40% less expensive than vCF and keeps 90% of its tensile strength while its modulus doesn't change [34], [35].

Chemical Recycling: In contrast to the mechanical and thermal processes, the chemical separation process, also known as solvolysis, is another fiber and matrix separation process. In this method CFRP waste is depolymerized via an appropriate solvent, i.e., a solvent dissolve the matrix, leaving behind clean CFs. The process parameters (pressure, temperature, and duration) and solvents (e.g., benzyl alcohol, glycol, catalytic solutions) vary on the type of matrix material.

Unlike pyrolysis, the embodied energy used in the solvolysis process is much higher [36]. Kooduvalli et al. [37] showed that in the pyrolysis process, an electric furnace

using renewable energy and natural gas requires 3MJ/kg and 41 MJ/kg respectively, whereas in solvolysis the deionized water and deionized water with acetone consumes 257 MJ/kg and 278 MJ/kg embodied energy respectively to separate the matrix and the fibers. On the other hand, the production of vCF uses around 198-595 MJ/kg whereas the rCF reclaimed via the chemical method required just 38 MJ/kg [38]. Another important factor to consider during recycling is fiber purity and sizing. The proportion of resin residuals left on the surface of the carbon fiber after recycling is referred to as fiber purity. In general, the CF recovered via pyrolysis and solvolysis yields fibers of varying purity. When compared to pyrolysis, the solvolysis recycling method outputs higher fiber purity [39]. The sizing on the carbon fiber plays an important role for the composite functionality. As a result, in the production of vCF a special type of sizing is applied with various compounds to protect and improve interfacial adhesion between CF and polymer during consolidation. The sizing is already present in the CFRP scrap material of type-1, but it is removed in types-2 and 3 after it undergoes pyrolysis and solvolysis process [40].

The recycling of CFs is just not enough to close the CFRP lifecycle loop (Fig. 2). Rather, CF recovered from sources that have reached the end of their useful life should be reprocessed for use in composites applications, e.g., the automotive industry. Hence, the reutilization of rCF should be the next step in the process [27].

2.3 – FIBERS MIXING TECHNIQUES

One of the most routine tasks in the chemical, industrial, and related sectors is mixing. When a system's composition, viscosity, temperature, etc. is not consistent throughout its volume, the technique employed to achieve this goal is called mixing. Moving ingredients from one region to another within a confined space is how mixing is accomplished. It may be useful for facilitating heat and mass flow, which is especially important when a system is undergoing a chemical reaction, but it can also be of importance on its own as a way of attaining a desirable level of homogeneity [41]. Although the chemical industry is responsible for the development of a significant portion of the knowledge on mixing, a huge number of other industries also engage in mixing operations on a bigger scale.



Figure 2: Closed loop recycling of carbon fiber composite- The CFRP components of a decommissioned aircraft, such as a Boeing 747, has around 30-40,000 lbs. of carbon fiber composites. The carbon fiber in these components is reclaimed via pyrolysis and similar processes. Carbon fiber is transformed into intermediary forms appropriate for composite manufacturing. The recycled carbon intermediate is then converted into a final composite part using resin transfer molding (RTM) or other processes. A final composite part is then installed on a vehicle- in this scenario a corvette part for under the hood [42], [43].

Hence, mixing is an important component of many processes in the pharmaceutical, food, paper, plastic, ceramic, and rubber industries [44].

The mixing mechanism is quite complicated because of the intricate nature and a large number of variables involved. For each mixing technique, a unique mechanism dictates the mixing rate and the feasible degree of mixing. When just a tiny amount of an active component has to be dispersed across a big batch of bulk solids or powders, the mixing quality, i.e., the degree of homogeneity, becomes critically crucial [45]. One such common issue that arises while mixing dry solid material is Segregation. The size, shape, and density of the individual parts of a mixture have a greater impact on the overall homogeneity of the final mixture. This issue has a negative impact on mixing techniques and is also common in several ways for solids sampling, packaging, transporting, and discharging [46]. There have been several efforts to categorize mixing challenges; for instance, Reavell et al. [47] utilized the finished product's flowability as a criterion for powder mixing. Another method of categorization might be based on the mode of operation, which could include batch, semi-batch, or continuous mixers, as well as in-line mixers, and so on. Furthermore, Harnby et al. [44] base their categorization on the phases that are present, i.e., liquid-liquid, liquid-solid, solid-solid, etc. This is arguably the best way to describe mixing since it enables the adoption of a cohesive strategy for dealing with issues that arise across many sectors [41]. The selection or design of the mixer and the way in which it operates are important factors to consider when mixing various types of particulate matter. Due to the nature of this work solid-solid mixing is discussed further in detail. The most common types of mixers used for mixing solid-solid matter are tumbler, hopper, high shear, fluidized mixers, extruders [48].

A tumbler mixer, a fully enclosed container that rotates on an axis, causes the particles inside the mixer to tumble over each other on the mixture surface. For example, when it comes to the horizontal tumbler cylinder, rotation may be achieved by positioning the cylinder on top of the driving rollers. For the most part, the vessel is supported on one or more bearings and connected to a driving shaft. In a tumbler mixer, the radial mixing occurs very quickly, but the axial mixing occurs more slowly and serves as the step that

controls the mixing rate. Therefore, tumbler mixers are more prone to segregation resulting in a nonhomogeneous mixture [48].

In a hopper mixer, particles move under the force of gravity, and the mixing is entirely driven by gravity flow. In order to provide a noticeable velocity gradient in the vertical direction without creating dead zones, a central cone is often placed in the hopper mixture. To achieve the desired degree of homogeneity, it may be necessary to recycle the particles from the outside, which would result in substantial axial mixing. Therefore, segregation is most likely to occur in this type of mixer as a result of percolation, both on the free surface of the hopper and throughout the bulk of the material [44].

Another type of mixer used for solid-solid mixing is high shear mixers. High shear mixers can be thought of as the mechanical replacement for the mortar and pestle. The majority of mixers involve some shearing of the powder, and as a result, there will be some displacement as well as mixing. High shear mixers are ideal for dispersing a bulk cohesive powder by breaking up small aggregates, as they apply a high and local nip or shear to the powder. The corn mill is a well-established high-shear mixer whose logical extension is the edge-runner mill, in which weighted rotating mill wheels shear the powder at the base of a stationary cylinder. The system works especially well when turning a poorly blended cohesive powder into a well-blended free-flowing aggregate [44].

The mixing in a fluidized mixer is caused by the passage of a gas through a bed of particles. In the fluidized bed, the particles are subjected to a stream of gas that flows upward against the direction of gravity. The buoyancy of the particles acts as a counterbalance to the weight that they contribute. Therefore, the mobility of each particle is greatly increased. If the volume of gas that is flowing through the bed is high enough, there will be a significant amount of turbulence within the bed, and the interaction of this turbulence with the mobility of the particles can result in very good mixing. When using a fluidized mixer, one of the inherent risks is that the constituent particles may readily segregate due to variable settling or projection rates if the turbulence is not completely achieved in the mixer [48].

Single- or double-screw extruders are frequently utilized in the plastics industry for mixing purposes. The feed to these units typically consists of the base polymer (in granule

or powder form) and various additives (such as stabilizers, colors, plasticizers, and so forth). During extruder processing, the polymer is melted, and the additives are combined. The extrudate is supplied from the extruder at high pressure and at a regulated pace for shaping using either a die or a mold. One of the challenges is that a substantial volume of heat is generated, and as a result of variations in temperature, the fluid property may alter by many orders of magnitude [41]. Figure 3 shows all the mixers discussed above.

To the author's knowledge, there is no known example of the mixing process or a piece of equipment that is directly used in the polymer composites industry to pre-mix different types of fibers which fall under the solid-solid mixing category. For e.g., mixing CFs with nylon fibers or mixing glass fiber with PP fibers. The literature found on powder mixing (solid-solid) is researched very well in the pharmaceutical industry. Therefore, for this work the mixing strategy used to mix different fibers was encouraged by powder mixing techniques used in the pharmaceutical industry.

A Resonant Acoustic® Mixing (RAM) is a unique ultra-fast mixing technique developed by Resodyn Acoustic Mixers that works by applying a high-intensity acoustic field with a low resonant frequency (60 Hz) in a non-contact manner to facilitate the mixing. Figure 4 illustrates the RAM mixing mechanism. In the RAM process, the fluid and a vessel can be explained as the mass-spring-damper system where energy is transmitted between the spring and the moving fluid mass. Unlike conventional mixing technology, where the mixing is focused at the tips of the impeller blades, the RAM technology for acoustic mixing works on the principle of generating micro-mixing zones in the entire mixing vessel, which facilitates homogeneous mixing. RAM technology works with several different material types, including liquid-liquid, liquid-solid, gas-liquid, and solid-solid systems. RAM technology is designed in such a way that there is fundamentally no loss of the mixer system’s mechanical energy into the materials being mixed created by the transmission of an acoustic pressure wave in the mixing vessel [49], [50]. RAM mixers come in few different designs and sizes based on the applications and overall production requirement. Figure 5a illustrates a compact benchtop LabRAM II mixer capable of handling 2.2 pounds of payload. Such mixers are ideal for lab scale

applications. Figure 5b shows an industrial scale RAM5 mixer for production scale batch mixing capable of mixing 80 pounds of material at a time.

2.4 –TEXTILE NONWOVENS USING RECYCLED CARBON FIBERS

After successfully reclaiming the rCF it often requires undergoing further processing into textile nonwoven intermediates to be used again in the composites industry. The key advantage of nonwoven preforms are outstanding economic feasibility due to high manufacturing output and considerable flexibility in terms of features such as areal density, uniform distribution, and degree of compaction [8]. The automotive industry places a significant importance on low cost and quick processing, making nonwoven preforms a perfect choice for automotive reinforced composites.

Numerous remanufacturing strategies for rCFRPs have been developed throughout the years. The manufacturing processes to process the discontinuous recycled fibers were adapted using established methods initially developed for virgin fibers, conventionally available as sized tows. In general, the technique that is used to manufacture the preforms causes nonwoven composites to display variable degrees of anisotropy i.e., the nonwovens are either aligned to some degree or randomly oriented.

Randomly oriented nonwoven composites minimize remanufacturing cost, but they also have lower attainable volume fraction and mechanical characteristics [4]. In Contrast, the nonwoven composites mechanical properties and molding conditions are both influenced by how well the fibers are aligned. According to some reports, the potential value of aligned rCFRP is up to thirty percent more than the value of randomly oriented rCFRP. Additionally, Gillet et al. [51] studied the impact of fiber alignment on the modulus and toughness of fiber reinforced composites, and they discovered profound effects of fiber alignment. Overall, highly aligned short fiber composites have great promise in the automobile sector; nonetheless, it is essential that mass production goals be met without significantly reducing characteristics [7], [52]. Randomly oriented nonwovens also known as Isotropic nonwovens have similar mechanical properties in all directions, can be manufactured using air-laid and WL methods. Conversely, anisotropic nonwoven textiles can be manufactured using carding process.

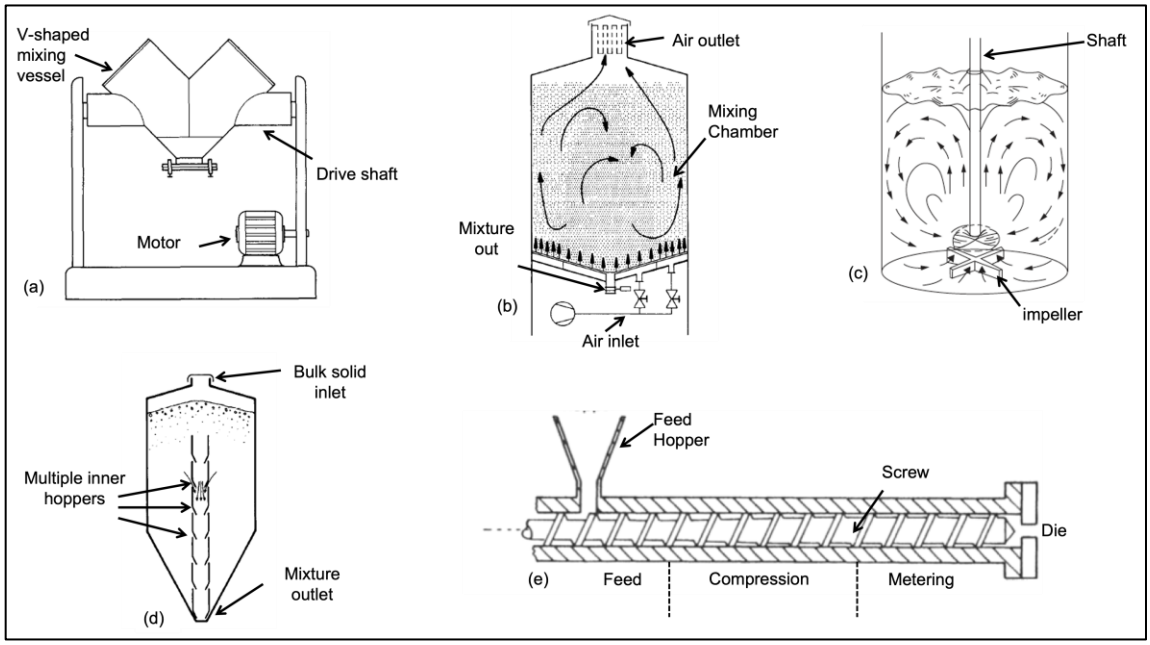


Figure 3: (a) V-Shaped tumbler mixer [48], (b) Fluidized-bed mixer [48], (c) High shear mixer [41], (d) Hopper mixer [48], and (e) Single-screw extruder [41]

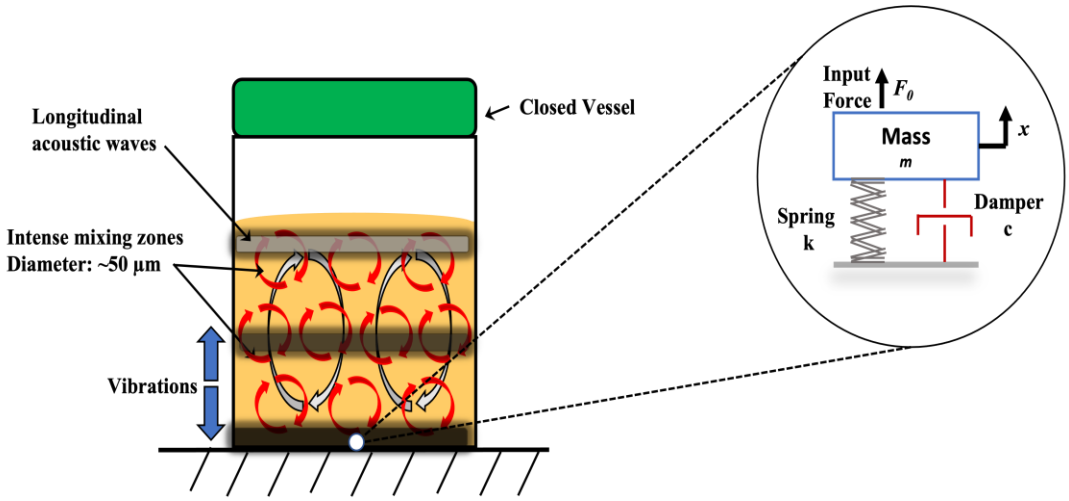
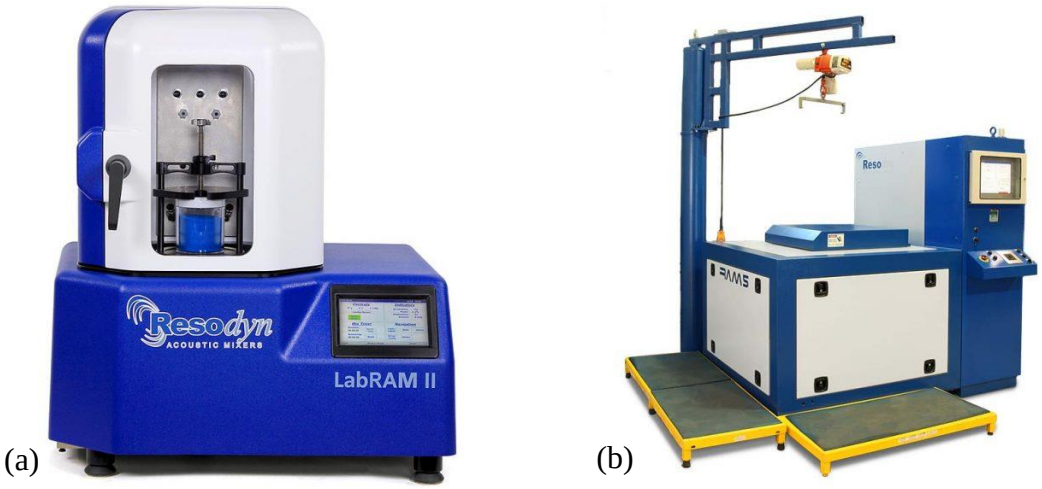


Figure 4: RAM mixing mechanism illustrating formation of micro mixing zones during the mixing process



(a) (b)

Figure 5: (a) A bench top LabRAM II resonant acoustic mixer with max payload of 2.2 pounds (Source: Resodyn Acoustic Mixers, Inc. [53]), (b) RAM5 mixer for production scale batch mixing capable of mixing 80 pounds of material at a time (Source: Resodyn Acoustic Mixers, Inc. [54])

2.4.1 ISOTROPIC NONWOVEN COMPOSITES

2.4.1.1. AIR-LAID

Air-laid is a dry laying technique in which individual fibers are evenly dispersed in an airstream and then directed toward a permeable screen or conveyor, where the fibers are deposited randomly in the form of a web. The resulting nonwoven mat is essentially isotropic in nature with a three-dimensional structure where the areal weight ranges from 150 to 200 g/m^2 [5], [11]. Figure 7 shows the schematic of Rando Webber air-laid process. Fiber separation is an integral aspect of the air-laid process and can significantly affect the homogeneity of the final nonwoven structure. In producing air-laid webs, it is crucial to ensure that fibers are opened and are free from clumps and entanglements before introducing them into the airstream. Hence, it is very critical to control the way fibers are introduced in the system to avoid any defects in the final nonwoven web structure. The following are some of the most effective ways to introduce fiber from the opening unit to the web-forming section: (a) free fall; (b) air suction; (c) compressed air; (d) closed air circuit; and (e) a combination of compressed air and air suction systems. The airlay techniques are very adaptable in the sense that they are compatible with a wide variety of fiber types and characteristics. This adaptability comes in part from the various air-laid machine designs and the concepts of fiber transfer and deposition utilized in airlaying. Like any other technology, air-laid process has its advantages and its limitations. The advantages include: (1) three-dimensional web structure with high areal density; (2) isotropic properties of resulting web; and (3) compatibility with a broad range of generic fiber types, such as natural and synthetic polymer fibers. On the contrary the main limitations are: (1) Fabric homogeneity depends heavily on fiber opening prior to web formation; (2) air flow irregularities next to the walls of the duct causes variability throughout the web structure; and (3) fiber entanglement in the airflow may cause web defects. In addition, the fiber length in air-laid ranges from 1-4 mm, which is far less than what could be accomplished by carding and WL processes [55]. To better handle the air-laid web it needs postprocessing method such as needle punching since air-laid process does not naturally entangle fibers as compared to other nonwoven manufacturing processes. Furthermore, the air-laid process

has slower rates of production which is slightly over 20 m/minute, which is substantially lower as compared to carding and WL techniques [5], [11].

The air-laid nonwovens industry uses variety of fiber types. Most of the air-laid nonwoven market is still driven by cellulose fibers made from wood pulp. In addition, natural polymer-based fibers (e.g., viscose rayon, Tencel) and synthetic polymer-based fibers (e.g., polyamide, polyester, polyolefins, and polypropylene) also contribute to the massive air-laid nonwovens industry [11]. To the author's best knowledge, a very limited work on carbon fiber or specifically rCF air-laid composites has been done.

Most recently, in 2020, Heilos et al. [10] at the Saxon Textile Research Institute (STFI) produced air-laid nonwoven composites using pyrolyzed rCF. For this work, they manufactured 300 grams per meter air-laid nonwoven preforms followed by needle punching process, and then infused them with epoxy using a wet compression method. The resulting nonwoven composite has a fiber volume fraction of 35%. The results showed that the tensile and flexural characteristics of the composite showed isotropic distribution as expected and exhibited high strength.

Processes utilizing woven recycled material are also briefly discussed in this section due to their commonalities to the air-laid technology Woven composites with a weight of 200 grams per square meter were developed by researcher Meredith et al. [56] at the University of Warwick using virgin carbon fibers prepreg and pyrolyzed recycled carbon fiber. Results indicated that despite considerable losses in tensile and flexural strength as well as interlaminar shear strength, rCF composites preserved strong tensile, flexural, and compressive modulus. Moreover, a comparison of recycled and vCF prepreg showed that the recycled material retained between 65% and 94% of its static characteristics and 94% of its specific energy absorption capacity. This is a crucial discovery because it demonstrates the viability of recycling CF for future usage in high-performance settings. In a similar manner, Pimenta and Pinho [57] at the Imperial College of London developed recycled woven composites and compared it with the virgin precursor. The composites were manufactured with 40-58% fiber volume fraction using resin film infusion method via vacuum or autoclave at high pressure. The results showed that rCF retained almost all

the strength and stiffness i.e., it showed excellent modulus retention. Despite this, tensile, compressive and shear strengths were all significantly reduced.

2.4.1.2 WET-LAID

The process of manufacturing WL nonwovens is similar to papermaking but with a few key differences. Figure 6 shows the schematic of the WL process. The fibers are mixed with water or a suitable solvent in this technique to form a fiber/water mixture. The mixture is then transferred to a head box where a continuous isotropic nonwoven web is formed. At this stage the water is drained from the web and is moved forward via a forming belt. Finally, the web is dried using the heaters and rolled up using a take-up system [5], [12], [55]. Natural or long synthetic fibers like cotton, hemp, or cellulose, as well as staple fibers, are the most prevalent types of fibers used in the WL process. In addition, the WL system has recently been implemented to manufacture CF nonwoven webs reinforced with thermoset or thermoplastic polymers [58]. The WL nonwovens have some significant characteristics, such as high productivity, uniform thin web preforms, recycled and hybrid fibers utilization, enhancement by fillers, and potential for in-line impregnation [59]. In addition, several factors affect WL nonwoven production rates, although reports have shown that they may reach as high as 1000 m/min [55].

On the contrary, there are some limitations in the WL process. The WL nonwoven textiles manufactured from water dispersed synthetic fibers are usually susceptible to defects. Therefore, the WL processed fibers must disperse well in water to produce a quality preform. The nonwoven preform may develop a wide range of defects if the fibers do not disperse adequately (due to various factors) or if they re-agglomerate after being dispersed. Such defects include fiber logs or sticks that fail to disperse in the agitation tank, dumbbell-shaped clusters of fibers caused due to insufficient flow design, and ropes that develop on a collecting screen before being entirely dispersed [60]. Furthermore, the web needs to be bonded to improve handling to make high areal density preforms.

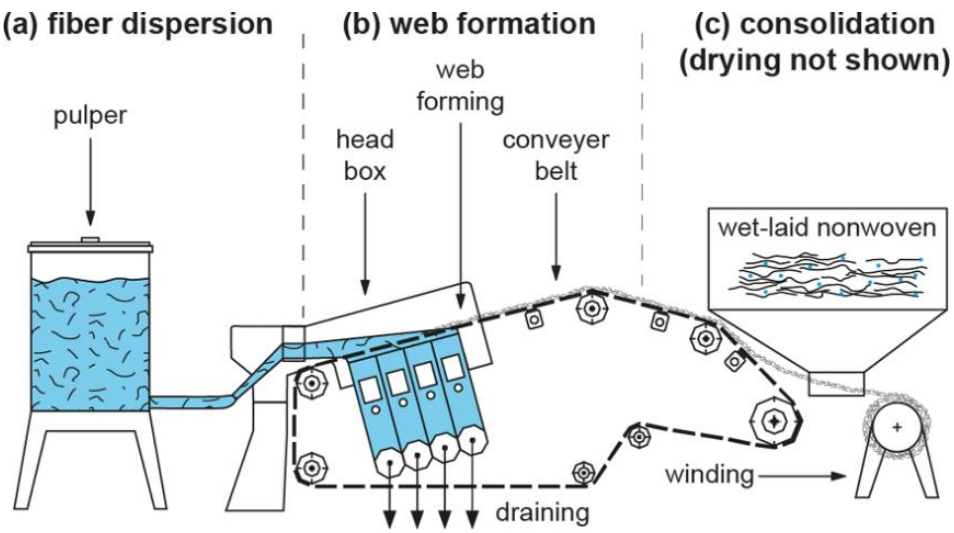


Figure 6: The WL process (adapted from [12]); (a) Fiber dispersion in water through mechanical mixing, (b) water drainage and nonwoven fiber web formation on conveyor belt, (c) consolidation of nonwoven fiber web into roll using take up system after drying.

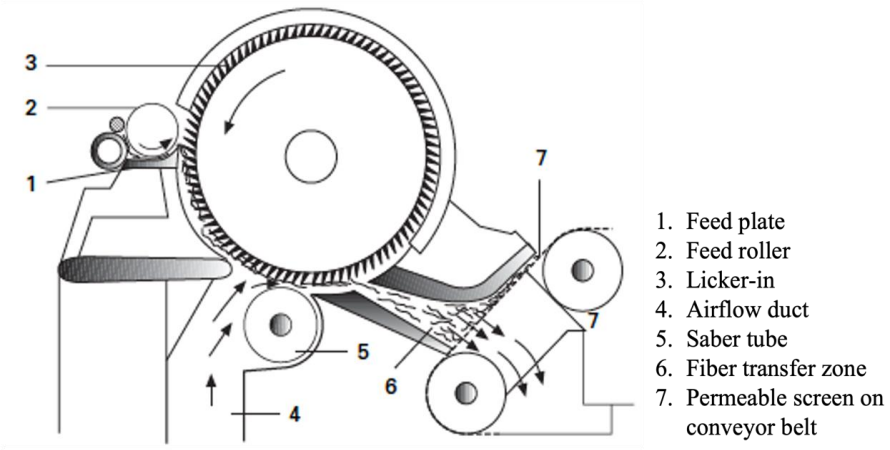


Figure 7: Air-laid process (adapted from [11]); Fiber mixture is fed using feed rollers where licker-in cylinder takes up the fibers. High velocity airflow removes the fibers from licker-in which forms a nonwoven fiber web on permeable screen on conveyor belt.

The most common nonwoven preforms bonding strategy developed is latex bonding, followed by hydrogen bonding, thermal bonding, hydroentanglement, and chemical bonding. WL nonwoven materials serve a variety of broad application fields, including the medical, apparel, textile, paper, and automotive industries [11].

It is important to note that most of the early work in WL nonwovens was done before the terminology "WL nonwoven" became widely used in the industry. At the University of Nottingham, Wong et al. [61] used compression molding to manufacture a recycled carbon fiber reinforced flame-retardant epoxy composite. A wet papermaking technique was used to manufacture a nonwoven mat with an areal density of 100 grams per square meter (gsm). The fibers were 12 mm in length and were molded to form a composite of fiber volume fractions ranging from 20 to 40% with a void content of 3-7%. They discovered that although the tensile and flexural modulus both increased with fiber volume fraction, the tensile strength peaked at 30% fiber volume fraction and declined after that. Heil et al. [62] from North Carolina State University used a resin transfer molding technique to manufacture rCFRP composite. The areal weight of nonwovens was targeted at around 1500 gsm made of 13 mm recycled T800S carbon fibers at 24% fiber volume fraction. One interesting result was that the compression strength of the composite was higher than the tensile characteristics. Typically, the unidirectional composites have higher tensile qualities than compressive ones due to fiber buckling effects. In this study, it was thought that the transverse direction fibers would act as a limiting factor to prevent the buckling of load-carrying, axially aligned fibers. At Fraunhofer institute, Wölling et al. [20], [21] manufactured rCF-PP composites via a commercial wet-laying process. Mechanical characteristics were studied concerning the impact of fiber orientation in the machine and transverse direction. The results showed that the tensile strength and modulus of the rCF-PP composite exhibited isotropic behavior in both the machine and transverse direction. Also, the ratio of mechanical characteristics in the machine and transverse direction was exceptionally close to 1. The reason for such behavior can be linked to the random orientation of fibers in nonwoven materials. Further, Szpieg et al. [5], [63]–[65], along with fellow researchers at Lulea University of Technology, manufactured a rCF reinforced modified polypropylene (rCF-rPP) composite material to study the effect of

strain rate on composites mechanical response. The intermediate nonwoven was created using papermaking techniques, with rCF dispersed in water to produce mats. Two layers of the rPP and three layers of rCF were stacked and compression molded into a consolidated composite panel with a thickness of around 1.20 mm and a fiber volume fraction of 40%. The results showed that the composite material they developed had poor stiffness compared to similar work done due to excessive fiber modulus degradation. Research by Wei et al. [66] and coworkers at the University of Tokyo evaluated compression molded thermoplastic composites made using a wet-laying technique and two distinct types of rCFs reinforced with polyamide 6 (PA6) and PP. Fabricated nonwoven preforms have a fiber volume proportion of 20%. Results revealed that PA6 composites outperformed PP composites on average, highlighting the importance of matrix characteristics in determining the performance of isotropic rCF composites. In addition, they demonstrated that combining various grades of rCF may alter composites flexural and Izod impact properties.

2.4.2 ANISOTROPIC NONWOVEN COMPOSITES

2.4.2.1 CARDING

Carbon fiber composites recycled are not often recovered as long, continuous fibers as their synthetic counterparts. Hence rCFs are in the form of chopped discontinuous fiber reinforcements. As discussed in the above sections, one way of processing rCF is to produce intermediate nonwoven mats. Specifically, in this section, the manufacturing of anisotropic nonwoven preforms via carding is discussed in detail. Carding is one such process that is most widely used in manufacturing nonwoven textiles from staple fibers.

Carding is a mechanical process aiming to disentangle the fiber stock into individual fibers to generate highly aligned nonwoven preforms with minimum fiber breakage. Carding works on a principle of fiber opening and layering actions carried out by toothed rollers present all over the carding machine. Hence, carding opens fibers, removes waste, and blends a variety of fibers thoroughly. For fiber types, wool, cotton, and polyester fibers are the most widely used fibers in the carding industry. One of the critical benefits carding offers is its ability to process various fiber types to manufacture products

with different characteristics. One illustration of this is the increased usage of recycled fibers in some nonwoven goods, such as automobile interiors. Recently, rCF has attracted the attention of the carding industry to manufacture highly aligned lightweight nonwoven preforms for usage in a variety of sectors, including the automotive, sports, and medical [11], [55], [67]–[69]

Figure 8 shows a schematic of an industrial-scale carding machine highlighting a typical fiber travel path through various components of the carding machine. The core elements of a carding machine include a taker-in, sometimes referred to as a licker-in, the main cylinder, workers, strippers, and the doffer cylinder. Every standard roller carder has the main cylinder, often known as a swift, typically the machine's largest cylinder. Around the main cylinder are smaller cylinders called workers and strippers, which typically function in pairs. The main cylinder is the most crucial part of the carding machine, which is the central distributor of fibers throughout its operation. A qualitative breakdown of how fiber is processed in the carding machine is discussed below [70], [71].

The taker-in, also known as the licker-in, is the first cylinder where the fibers meet. In this zone, the fiber tufts are opened, and the pins on the revolving licker-in grab the fiber and transfer them to the main cylinder. Subsequently, the fibers are transferred onto the main cylinder, and further, it gets transferred into the carding zone where most of the processing occurs. In carding zone, the workers and strippers work simultaneously in contact with the main cylinder to achieve the necessary stripping and blending of the fibers. The continuous action of workers and strippers also avoids fiber overloading in the overall process. Finally, the fibers from the main cylinder are stripped off by the doffer cylinder in the doffer transferring zone, and hence the fiber exit the system in the form of a unidirectional nonwoven preform. The remaining fibers spin around the cylinder's surface until they once again reach the doffer transfer zone, and this procedure is repeated until all fibers have transferred [11], [71]. Further, the carded nonwoven preform needs to be bonded using the methods described in the air-laid and WL section to improve the

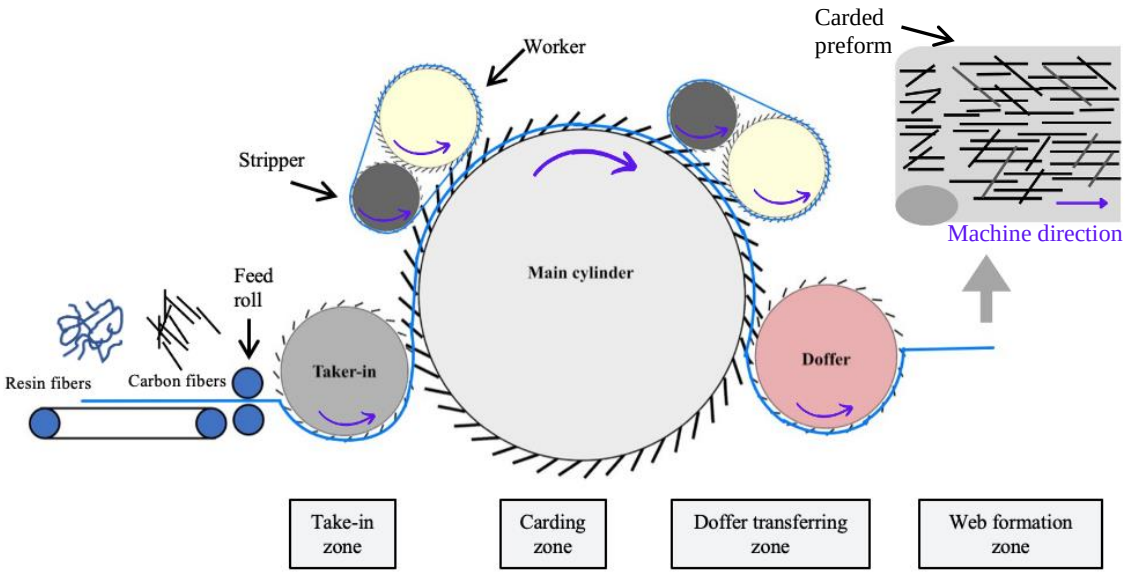


Figure 8: Carding process schematic (adapted from [7]); The fiber mixture is fed via feed rollers where taker-in takes up the fibers and transfers onto the main cylinder. In carding zone, the worker and stripper work simultaneously with main cylinder for stripping and blending of fibers. In doffer transfer zone, the fibers are stripped off from main cylinder via doffer cylinder resulting in a nonwoven carded preform in web formation zone.

handling of nonwoven preforms. The most common method to improve the handling of carded nonwoven mats is needle punching. The needles from the needle punching machine create a frictional interface with the adjacent fibers, which results in the formation of a permanent bond among the fibers in the nonwoven mat [8], [15].

Carding quality is determined by several interrelated factors, including but not limited to fiber loadings on carding elements, fiber transfer rate, fiber mixing action, and fiber breakage. In the last 100 years, several efforts have been made to develop mathematical models and measurement systems to understand the parameters mentioned above for effective carding. One such vital parameter to consider is the fiber loading on carding cylinders. Several models have been created over the decades to help design modern fast carding machines. Krylov et al. [72] examined how machine settings affected fiber loading on a flat-top card cylinder. The empirical formula is given in Equation 1 [72]. In this equation, fiber loading on the flat cylinders was ignored.

$$Q_c = \frac{R_c P}{3.6 v_c}\left[\frac{2\pi 100 + \eta[\alpha(c-1) - \beta]}{\eta}\right] \quad (1)$$

where Q_c is the total fiber loading on the cylinder (grams), R_c is the cylinder radius (m), P is the productivity of the carder (kg/h), v_c is the cylinder surface speed (m/min), η is the doffer cylinder collecting power, c is the waste index, α is arc angle between the licker-in and the flats (radius), and β is the arc angle between the doffer and the licker-in (radius). According to the findings derived from equation 1, an increase in the surface speed of the cylinder led to an increase in the fiber collecting power of the doffer and a reduction in the fiber loading on all card components.

Fiber transfer between cylinders is another essential parameter to consider in carding. The main cylinder and doffer interaction are important in carding since doffer cylinder speed settings play an essential role in producing a uniform web structure. Baturin et al. [67] investigated how changing the machine's settings affected fiber transmission between the cylinder and doffer on a flat-top card. Equation 2 provides doffer's collecting power using data from experiments and preceding theoretical analyses:

$$\eta = \frac{v_D K_1 K_2 K_3}{v_C K_\omega + v_D K_1 K_2 K_3} \quad (2)$$

where v_D and v_C are the surface speed (m/min) of doffer and main cylinder respectively.

$$K_1 = \frac{N_{c,d}}{N_{c,c}} \quad (3)$$

$N_{c,d}$ and $N_{c,c}$ are pins per unit area of doffer and main cylinder respectively, K_2 is a coefficient relating the angles of inclination of the teeth of the cylinder and doffer carding cloth to the ratio of entrapment powers, K_3 is coefficient describing the ratio of cylinders fiber capacity of the interacting card clothing surfaces, and K_ω is coefficient of centrifugal force due to cylinders rotation on cylinder load. The effect of the setting distance between the cylinder and the doffer is not taken into consideration in equations 2 and 3.

As stated, carding is a well-known method of producing highly aligned nonwoven preforms. Nearly a decade ago, carding emerged as a prominent technique in the field of nonwoven CF composites. Since then, a considerable amount of research has been carried out globally to make the most of the carding process to capitalize on the enormous potential that highly aligned short fiber composites hold within the automotive sector [73]. The composite's mechanical properties and molding process are influenced by how well the fibers are aligned [27]. According to some reports, the potential value of aligned rCFRP is up to thirty percent more than that of randomly oriented rCFRP. Additionally, Gillet et al. investigated the impact of fiber alignment on the modulus and strength of CFRPs and discovered substantial impacts of fiber alignment [51]. On the contrary, the continuous action of carding teeth on the fibers during its operation comes at the cost of fiber breakage. Therefore, to successfully card rCF fibers on a carding machine, the machine is modified accordingly to minimize fiber attrition. One of the primary objectives of recycling is to maintain the fiber length for as long as possible to allow for several recycling cycles and, as a result, contribute to a complete circular economy. Additionally, longer CFs can significantly enhance the composite's mechanical properties. Therefore, the minimum fiber length should be around 30 mm before processing them in the carder since the fiber length is drastically reduced in the nonwoven manufacturing process. [8]. Shao et al. [1] at Donghua University in China manufactured highly aligned thermoplastic nonwoven

composite by carding 50 mm carbon fiber with PP fibers. The findings demonstrated that the carbon fiber breakage could be minimized during the carding process by adding friction-reducing oil, increasing the distance between the cylinder and rollers, and varying the cylinder speed. In 2021, Manis et al. [8] from the Fronhofer institute manufactured carded nonwoven composites using rCF reinforced with Polyamide 6 (PA6) and Polyethylene terephthalate (PET) fibers. It was found that rCF underwent more fiber breakage, and it was demonstrated that fewer worker-stripper pairs resulted in less fiber attrition. Additionally, they discovered that the mechanical qualities of PET fibers were superior to PA6, which is truly remarkable given the widespread use of recycled PET. Hence, it was concluded that fiber breakage and fiber alignment are a trade-off in the carding process. The number of worker-stripper pairings is directly correlated with the degree of fiber orientation in the nonwoven preform.

In order to accelerate the circular economy efforts of CFRPs, rCF composites along with thermoplastic matrix offers great recyclability and reusability since thermoplastic polymers have a rapid molding cycle and are easy to shape [7]. At the University of Tokyo, Xiao et al. [7] duplicated rCF using vCF by removing the sizing. The 50 mm long fibers were blended with thermoplastic polyamide fibers to create a carded, nonwoven preform. Further, a stretching process was introduced before compression molding to improve the fiber alignment on carded mats, leading to a higher fiber volume fraction. The results showed that the tensile and flexural properties of stretched nonwoven carded composites were similar to those of unidirectional CF-reinforced thermoplastic tape. They also showed that carded rCF composites had a high degree of fiber alignment within ±15º. Heilos et al. [10] at STFI produced carded nonwoven composites using pyrolyzed rCF. For this work, they manufactured 300 grams per meter carded cross-lapped nonwoven preforms followed by a needle punching process. They then infused them with epoxy using wet compression and resin transfer molding. As expected, the results showed that carded composites yielded higher tensile properties in the machine direction than in the cross direction. Also, it was found that higher fiber content in the composite resulted in more anisotropic behavior. Additionally, they recycled the rCFRP to make rrCF (re-recycled nonwoven carbon fiber

composites) to show that rCFRP composites can be recycled repeatedly. The rrCF showed only minimal loss of properties when compared to rCFRP.

Much research has been done on rCF carded composites considering different parameters such as varying rCF length, reinforcing matrix material, different carding machines and parameters, final part manufacturing techniques, etc. This work uses a unique approach to preparing rCF thermoplastic nonwoven composites. A unique RAM mixing technique is used to achieve homogeneous rCF-PP fiber mass, which is a critical step before processing the fibers in a carding machine. To the author's knowledge, nowhere in the literature review is found that any two different fiber types are homogeneously pre-mixed before being carded. Further, the literature review shows that the minimum length required for carding of rCF is around 30 mm. In this study, carded and WL composites made of rCF (5 mm in length) and PP (6.35 mm in length) are manufactured by compression molding so that the characteristics of anisotropic carded composites can be compared to those of isotropic WL composites.

CHAPTER 3- MATERIALS AND METHODS

3.1 MATERIALS

The rCFs (Carbiso^{TM} C IM56P) used in this work were provided by ELG Carbon Fiber Ltd. (U.K.) which are recovered via a modified pyrolysis process by ELG. According to the manufacturer, the rCF received was unsized since the sizing was entirely removed in the pyrolysis process. The reclaimed rCF used throughout this work were un-sized. The length of the rCF was between 3 and 10 mm, with a mean fiber length of 5 mm. Figure 9 shows the as received rCF.

Polypropylene fibers (PP) were chosen as the matrix fiber to be used with the rCF since this polymer is frequently utilized as a cost-effective matrix material for thermoplastic composites. MiniFibers Inc. (Johnson City, U.S.A.) manufactured and delivered the fibers in staple form (6 mm length, 1.65 dtex fineness). The detail of rCF and PP is summarized in Table 0.1.

3.2 FIBERS MIXING TECHNIQUE

The resonant Acoustic Mixing (RAM) process (Resodyn Acoustic Mixers, Montana, USA) was used to mix rCF and PP fibers as dry bulk homogeneously and in two different liquid solvents. A scope test was performed using rCF fibers to determine the fibers mixing behavior and mixing parameters. Table 0.2. shows different mixes based on the overall fiber weight used in the vessel for a given mix. Five different types of mixing were performed, as shown in Table 0.3 to find the best mixing strategy to achieve a homogeneous rCF-PP mixture for the overall study. Figure 10 and Figure 11 shows the homogeneous mixture of rCF-PP fibers after being processed in the LabRAM II system. The rCF and PP fibers were mixed at a 30:70 weight proportion for this work.

3.3 ANISOTROPIC NONWOVEN MANUFACTURING VIA CARDING PROCESS

After the rCF-PP fibers are homogeneously premixed, as shown in Figure 11, they were processed via a two-cylinder lab scale hand carding machine to obtain an anisotropic nonwoven preform. In this work, two hand carding machines (supplied by Brother drum

carder, U.S.A.) were used with different specifications for producing nonwoven mats. Both are described in detail in the following sections.

3.3.1 STANDARD DRUM CARDER (CARDER 1)

The Brother carder 1 is 12” wide, 24” long and 9” tall, producing a 9” x 22” batt. It is a right-hand adjustable coarse carder with 72 TPI (teeth per inch), i.e., 72 pins on a carding cloth per square inch. The carder 1 machine is shown in Figure 12.

The carder 1 machine consists of several parts such as a small cylinder called a licker-in drum, a main cylinder also known as swift, a poly belt, copper bushings and a rotating handle. The fibers mixture is fed to a licker-in cylinder. The function of licker-in drum is to take up the fibers and transfer it to the swift cylinder. The licker-in drum serves a dual purpose in creating a parallel stack of fibers on the swift cylinder: first, it brings the fibers into contact with the pins of the swift cylinder, and second, it retains the fiber as it rolls onto the swift cylinder, allowing it to gradually align in the machine direction. The swift cylinder rotates faster than the licker-in cylinder and this difference in speed results in a uniform nonwoven mat. The poly belt’s primary function is to exert tension on the pulleys and transmit power from carder handle to rotate the cylinders. Another essential function of a poly belt is to absorb unexpected shocks and blockages resulting from fiber clumps passing between rotating cylinders.

3.3.2 DELUXE BABY DRUM CARDER (CARDER 2)

Unlike carder 1, the design of carder 2 is quite similar, with few key differences. The carder 2 is 7” wide, 20” long, and 14” tall and weighs around 14 pounds. It can produce 5”x22” batts. It is also a right-hand coarse carder with 72 TPI. This carder has a brush attachment that can be removed from the top of the frame and makes direct contact with the swift cylinder. The function of the attached brush is to keep the fibers intact while carding, which ultimately results in a uniform nonwoven preform. The critical difference in this carder is that the swift cylinder is 4” wide, whereas in carder 1 it is 9.5” wide. The diameter of the swift cylinder in both the carders is 7”. Another critical difference in both the carders is the pin length. carder 1 has stainless steel pins of ½”, whereas carder 2 has 5/8” long pins. Carder 2 is shown in Figure 13.



Figure 9: As received rCF from ELG Carbon fiber Ltd. (Mean fiber length ~ 5mm)

Table 0.1: rCF and PP material specifications

Material	Manufacturer	Code	Tensile Strength	Tensile Modulus	Specific gravity (g/cm^3)
rCF	ELG	Carbiso^{TM} C IM56P	4100 (MPa)	259 (GPa)	1.8
PP	MiniFibers	PPSTD-070NRR	2.5-3.8 (cN/dtex)	-	0.90

Table 0.2: rCF-PP fibers mixing outline

Material	Weight (%)	-	Mix 1 (gm)	Mix 2 (gm)	Mix 3 (gm)	Mix 4 (gm)	Mix 5 (gm)
Recycled Carbon Fiber	30	Scoping Test	15.00	7.5	3.75	3.75	3.75
Polypropylene	70	-	35.06	17.50	8.75	8.75	8.75

Table 0.3: rCF-PP mixing with different parameters using LabRAM II

Mixes	Polystyrene vessel size	Time (min)	Acceleration (g)	Temp before (°C)	Temp after (°C)
-	Scoping test (Only rCF) fibers 16 oz	2	100	18.4	19.4
Mix 1	32 oz	1	75	18.4	-
		2	100	-	20.1
Mix 2	32 oz	3	100	18.4	24.2
Mix 3	32 oz	5	100	18.4	22.7
Mix 4	300 ml water 32 oz	1	100	18.4	21.0
Mix 5	300 ml isopropanol (IPA) 16 oz	1	100	18.4	18.6



Figure 10: Before mix 4: rCF and PP fibers in water before RAM

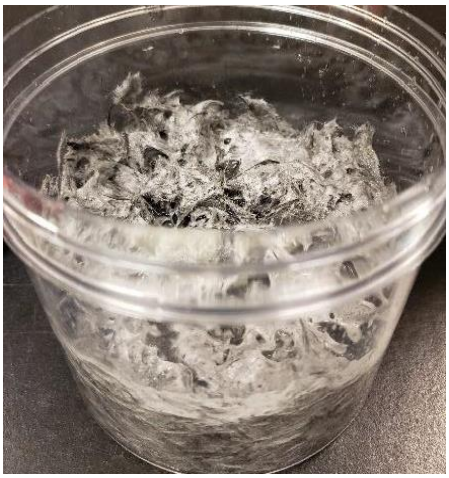


Figure 11: After mix 4: Homogeneous rCF-PP fiber mixture after RAM

3.3.3 rCF-PP NONWOVEN PRODUCTION PROCESS

The carding process can be divided into three stages: feeding, carding, and removing. Before processing the material in the carder, the rCF-PP fiber mixture was dried in the conventional oven for 6 hours at 80 ºC to remove the moisture content. The entire process of rCF-PP nonwoven production using both the carders is shown in Figure 14 and Figure 15.

1. Feeding
    a. First, the carding machine is positioned on a sturdy table with the help of a few clamps, so it does not displace when operational.
    b. The dried rCF-PP mixture was fed slowly across the small drum by rotating the carder handle clockwise.

Note: To ensure that the fibers on the licker-in are dispersed uniformly, it is essential to remember that the fiber mixture must be distributed equally over the carder feeding zone.

2. Carding
    c. As the fibers are fed continuously, the small drum keeps taking up the new fibers until it gets full.
    d. In this process, the fibers were continuously sprayed with water using a mist spray bottle so that the rCF fibers did not fly out due to their short length when processed between the drums.
    e. After the small drum is fully saturated with fibers, the pins on the large cylinder start to pull fibers apart from the small drum. This is a critical step in the production of the nonwoven preforms. As the fibers are transferred onto the big drum, the unique arrangement of the metal pins on the carder tries to align fibers in machine direction.
    f. This process is continued until the big drum is covered up entirely by the fibers slightly below the metal pins.

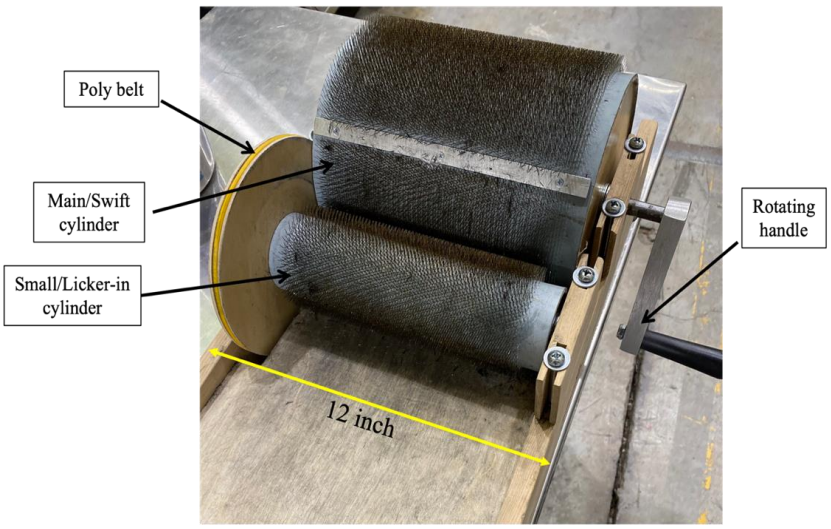


Figure 12: Manual standard drum carder (carder 1) with two cylinders. Main cylinder (width 9.5 in., diameter 7 in., pin length 0.5 in., and 72 TPI (teeth per inch)

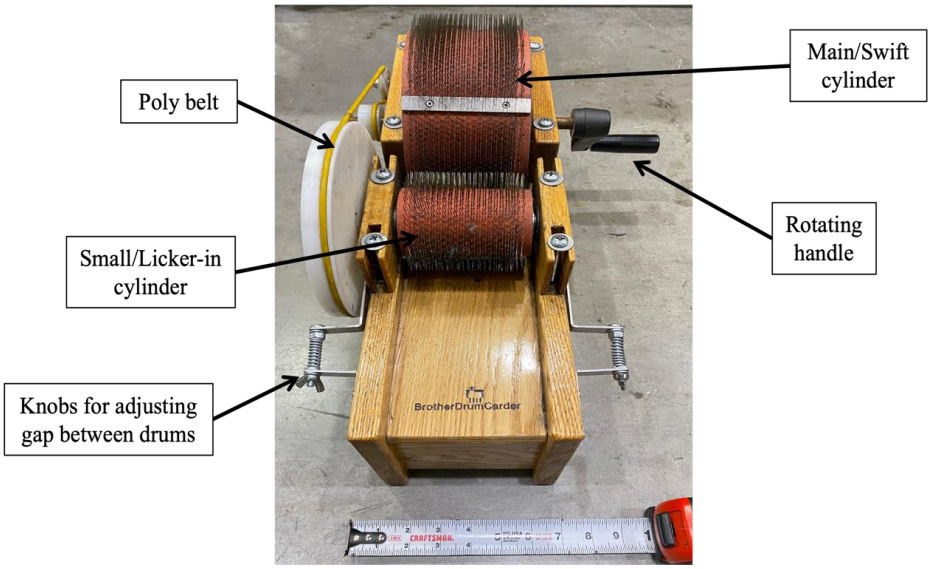


Figure 13: Manual deluxe baby drum carder (carder 2) with two cylinders. Main cylinder (width 4 in., diameter 7 in., pin length 0.625 in., and 72 TPI (teeth per inch))

3. Removing
    g. At this stage, the big drum, i.e., the swift cylinder, is full of fibers.
    h. A brush is used to separate the nonwoven web from the carder. The brush is held firmly against the pins, and the handle is slowly rotated in a counterclockwise direction.
    i. The brush lifts the nonwoven batt slowly until a desired nonwoven mat length is obtained.
    j. Finally, the nonwoven mat is dried in an oven in an aluminum tray at 80 ºC for 3 hours.

There is a slight variation in the production of nonwoven carded mats using both carders. The key differences are highlighted as follows:

i. Before feeding the fibers in a carder 1, both drums were covered by Peel Ply fabric, as seen in Figure 14a. Peel Ply plays a major role in removing the nonwoven mat at the end of carding operation. The rCF-PP nonwoven mat is obtained by first removing the peel ply fabric and then detaching the mat from the fabric.
ii. Peel Ply is required for carder 1 only and not for carder 2. The swift drum on the carder 1 is 9.5” in length. The starting mean length of the rCF in this study is 5 mm which is considered very short to be even carded at first place. Consequently, the nonwoven preforms produced on carder 1 becomes difficult to remove without peel ply. On the contrary, the width of the swift cylinder on deluxe carder is 4”. The nonwoven made from this carder is around 4.5” wide. Hence, it is easy to remove and handle the nonwoven mat manufactured from carder 2.
iii. The two carders also have distinct differences in terms of their designs. Carder 2 has a special, removable brush head mounted on top of the frame. The brush helps comb the fibers in the direction it is carded, resulting in uniform nonwoven rCF-PP mats.

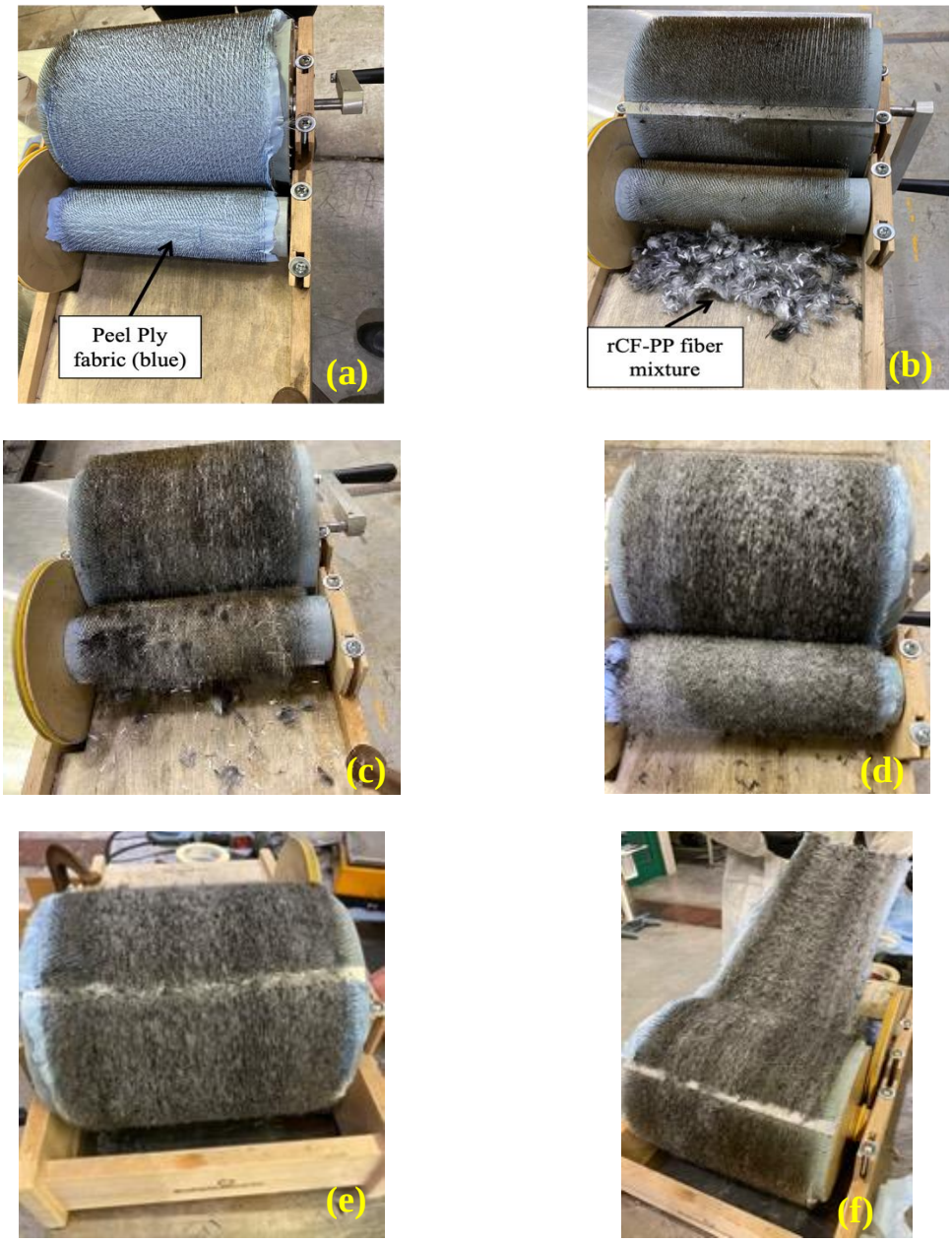


Figure 14: Manufacturing rCF-PP nonwoven mat using carder 1; (a) Both drums covered with peel ply fabric, (b) rCF-PP fiber mixture fed to licker-in cylinder, (c,d,e) carder drums covered with fibers after continuous carding, and (f) removal of nonwoven rCF-PP carded mat with supporting peel ply fabric.



Figure 15: Manufacturing rCF-PP nonwoven mats using carder 2; (a) rCF-PP fibers fed to licker-in cylinder, (b,c) carder drums covered with fibers after continuous carding, (d) rCF bundles collected on fiber catching tray during carding, (e) nonwoven rCF-PP carded mats.

3.4 ISOTROPIC NONWOVEN MANUFACTURING VIA WET-LAID PROCESS

WL is another process used in this work to manufacture isotropic nonwoven mats. The rCF-PP WL nonwoven mats were produced using an innovative mixing method [74] in a hand sheet WL tank (Adirondack machine corporation, U.S.A.), as seen in Figure 16. The tank is a 12”x12” stainless steel box that stores 30 liters of water. The top of the tank is equipped with a couple of stirrers that help mix fibers. The bottom of the tank has a removable stainless steel forming mesh to collect the final nonwoven mat.

3.4.1 WL rCF-PP NONWOVEN PRODUCTION PROCESS

The dried rCF-PP fibers, along with 2.0 g of dispersant (Alkyl amine surfactant Nalco 8493^{TM}) and 2.0 g of viscosity enhancer (anionic flocculent Nalclear 7768^{TM}) are added to the water in WL tank. The fibers were mixed for 10 minutes, and the water was drained through a fine mesh leaving behind a rCF-PP nonwoven mat (12”x12”). The prepared nonwoven mat was targeted to get an areal weight of around 280 gsm (g/m^2) is seen in Figure 17. The excess water was soaked out of the mat using a vacuum machine, and then the mats were placed in a drier (Emerson Speed Dryer-Model 145) at 200 F for 20 minutes to dry. The mats were trimmed to 11” x11” size for compression molding. Finally, the carded and WL rCF-PP nonwoven mats were prepared for compression molding to get a consolidated composite panel for further study.

3.5 COMPRESSION MOLDING

rCF-PP nonwoven carded, and WL mats were fabricated into a consolidated flat composite panel via a heated compression molding Carver press (Model 3895). Due to the different sizes of the nonwoven mats, two different steel molds were used. 6” x 6” mold was used to fabricate carded nonwoven mats, whereas an 11” x 11” mold was used for WL mats. The carded composite plates were fabricated by placing the mats in two arrangements: Unidirectional and 0º/90 º cross-ply layup. The carver press settings for both carded and WL compression molded panels are outlined in Table 0.4.

PP has a low melting point, at around 160 ºC. This information, along with differential scanning calorimetry (DSC) and thermogravimetric analysis (TGA) results, was used to establish the processing conditions to get well consolidated rCF-PP panels as shown

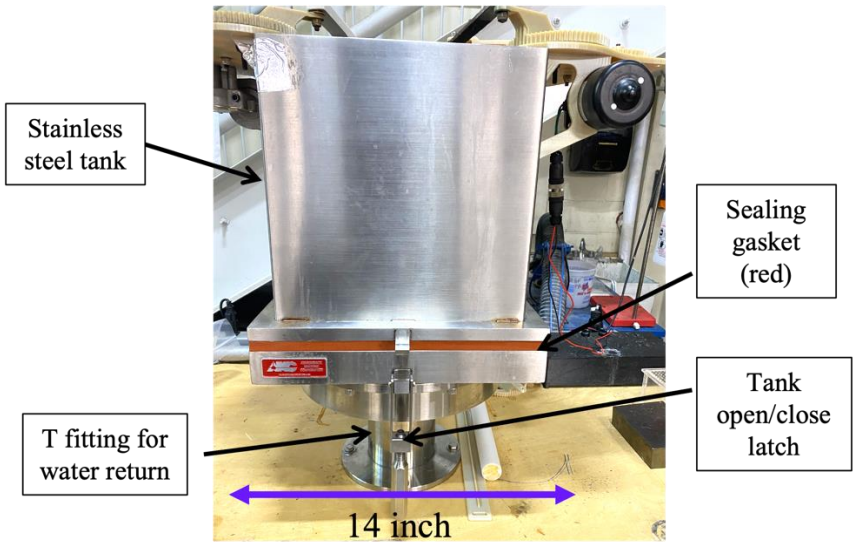


Figure 16: Lab scale WL mixer

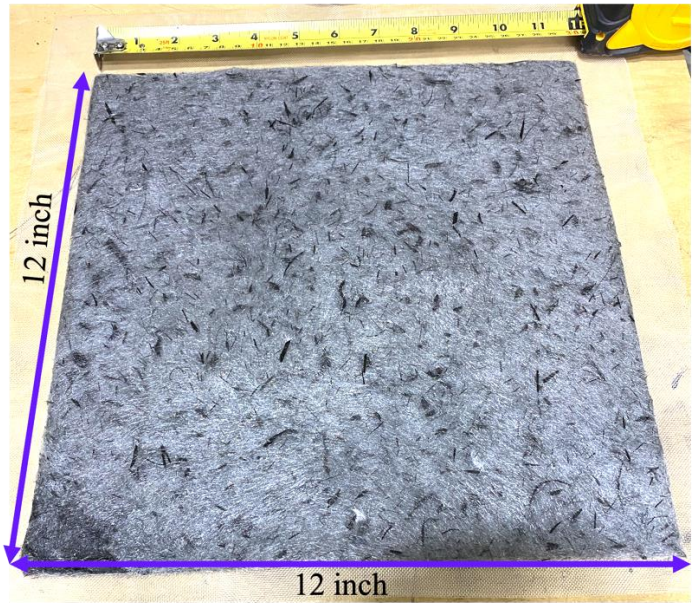


Figure 17: Isotropic rCF-PP nonwoven WL mat (12 in. x 12 in.)

in Figure 18. A total of 14 layers of carded nonwoven mats were layered in the mold, whereas for WL, a total of 9 layers were stacked to achieve a 3 mm thick plate. Similarly, a neat PP plate was made using similar processing parameters as carding composite plate.

3.6 FIBER LENGTH DISTRIBUTION (FLD)

A burn off test was conducted on the rCF-PP carded nonwoven mats to remove the PP polymer and recover the carded rCF fibers, thereby evaluating the relation between fiber breakage and mechanical properties following carding. The effect of pin length on fiber breakage was investigated using mats made with both carders. A carded rCF-PP mat (Figure 19a) wrapped in aluminum foil was placed in an aluminum tray inside the box furnace (Thermo Fisher Scientific, Model # BF51728C-1, Waltham, MA), at 400 °C for 4 hours [75]. The rCF were left behind in a clumped fiber bundles after the PP matrix were completely burned off (Figure 19b). Fiber bundles must be separated into single fiber filaments to measure the effective length. For the FLD study, two methods were used to separate fiber bundles: 1) the tweezer method and 2) the ultrasonic method. In tweezer method, the fiber bundles were separated physically with the plastic tweezer and collected on a white piece of paper, later scanned under a scanner (Canon Canoscan LiDE 400, 4800 dpi) to record the image. At least 1500 single fiber filaments were measured manually in ImageJ software (version 1.53a, bundled with Java 1.8.0_172). In ultrasonic method, the rCF fiber bundles were put into a glass vial with an acetone solution. The glass vial was submerged into an ultrasonic bath (Fisher Scientific, Waltham, MA) for a few seconds until fiber bundles were separated into fine individual fibers. Then the solution was immediately pipetted out and poured on a microscopic slide (2in. x 2in.), so the acetone could evaporate. After the evaporation of acetone, the fibers were imaged using a VHX-5000 digital microscope (KEYENCE Corporation, Itasca, IL) [76] (Figure 19c). Then the fibers were measured using a python script in ImageJ software [77]. At least 1500 fibers were measured for each sample and method type.

Table 0.4: Carver press parameters for rCF-PP

	Pressure (ton)	Time (minutes)	Temperature (°C)
Carding	0.5	30	185
	1	3	
	1.4	3	
	1.8	30	
WL	1.7	30	
	3	3	
	5	3	
	6.5	15	



Figure 18: Compression molded rCF-PP panels. (a) Unidirectional carded panel (30% fiber weight fraction, panel thickness: 2.9 mm), (b) Isotropic WL panel (30% fiber weight fraction, panel thickness: 2.8 mm)

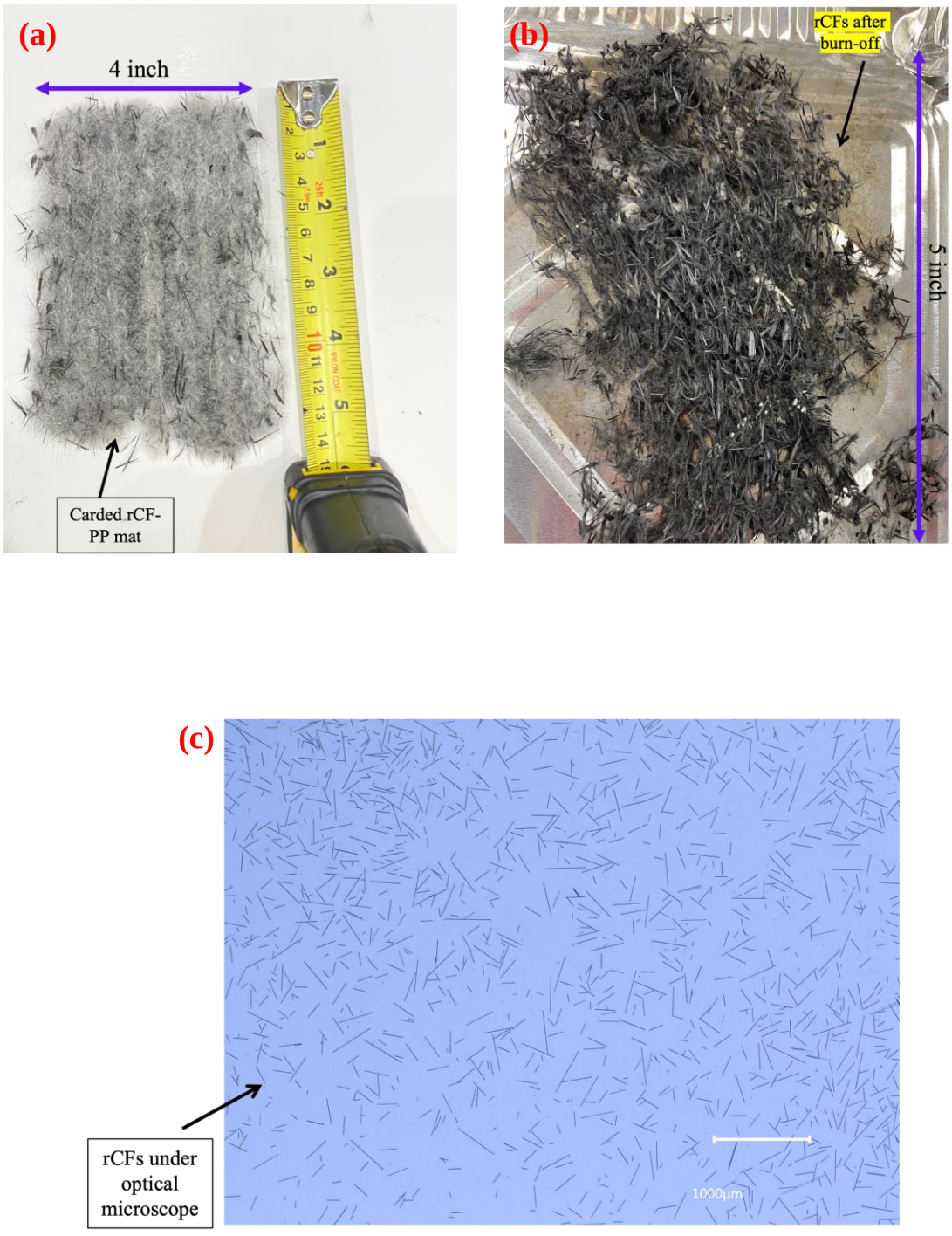


Figure 19: (a) rCF-PP mat before burn-off; (b) rCFs after burn off, and (c) Optical image of rCFs under microscope after separating the fibers from bundles via ultrasonic method

3.7 MECHANICAL CHARACTERIZATION

3.7.1 FLEXURAL TESTING

The flexural properties for the specimens were measured per ASTM D790 standard [78], using a Test Resource frame (Model #: 313, MN, USA) with a 50-kN load cell. Five coupons were prepared from a compression molded rCF-PP panel of each type. The flexural specimens (75 x 15 x 3.75 mm^3) were loaded at 1.6 mm min^{-1} with a span length of 60 mm.

3.7.2 INTERLAMINAR SHEAR STRENGTH TESTING

The Interlaminar shear strength of rCF-PP composite samples were measured per ASTM D2344 standard [79] using a Test Resource frame (Model #: 313, MN, USA) with a 50-kN load cell. Similarly, to the flexural test, five coupons were prepared from a compression molded rCF-PP panel. The ILSS specimens (22 x 7.5 x 3.75 mm^3) were loaded at 1.0 mm min^{-1} with a span length of 15 mm.

3.7.3 IZOD IMPACT TESTING

A Tinius Olsen IT 504, with a 22.6 J loading capacity and a 37 N pendulum weight, was used to conduct the Izod impact test per ASTM D-256 [80] in order to understand the amount of stress a material can absorb before it breaks. Five specimens from each panel were extracted, measuring 64 mm x 12.7 mm. Specimens were made using a notch type A with a radius of 0.25 mm and a notch angle of 45º. The notch on the Izod samples were machined on HAAS (VM-3) with a custom 3D printed Izod specimen holder.

3.7.4 TENSILE TESTING

A tensile test was conducted as per ASTM D638-Type 1 standard [81] to investigate the degree of fiber alignment on carded specimens compared to isotropic WL specimens. The test was performed on a Test Resource frame (Model #: 313, MN, USA) with a 50kN load cell and a constant crosshead speed of 2mm/min. The strain data was calculated using an extensometer (Model:3542, Epsilon Technology Corp, WY, USA) with a gauge length of 25.4 mm. Five dog bone samples from each panel type were prepared with a gauge length of 50 mm.

3.8 SCANNING ELECTRON MICROSCOPY (SEM)

SEM was performed to investigate the fiber alignment, fiber-matrix interfacial bonding, and fiber pull-out in carded unidirectional and WL fractured tensile composite specimens. Before scanning, the specimens were spluttered with gold particles to avoid charge build-up on composite samples during imaging The SEM equipment used was Phenom XL (ThermoFisher Scientific PW-100-018), with a low voltage of 10 kV.

3.9 DIFFFERENTIAL SCANNING CALORIMETRY (DSC)

The thermal behavior of the rCF-PP composite was characterized by using Q2000 (V24.11 Build 124) DSC instrument. The samples were subjected to heat/cool/heat cycles in the range of 40 ºC to 220 ºC in the presence of nitrogen gas set at 50 mL/min. First, the samples were heated to 220 ºC and kept there for 2 minutes to remove the thermal history. Next, they were cooled to 40 ºC at a rate of 10 ºC/min and then subjected to another heating cycle to 220 ºC at a similar rate to attain the melting peak. Due to semi-crystalline nature of PP polymer, the degree of crystallinity (X_c) was obtained using Equation 4.

$$X_c = \frac{\Delta H_m}{\Delta H^\circ} \text{ x } 100\% \quad (4)$$

Where ΔH_m is the melting enthalpy of the material (J/g) which is given by the area under the melting peak, and ΔH° is the melting enthalpy value of 100% crystalline phase of PP polymer, which is assumed to be 209 J/g [82].

3.10 THERMOGRAVIMETRIC ANALYSIS (TGA)

TGA was performed on rCF-PP compression molded samples using Q50 (V6.7 Build 203) TGA instrument (TA Instrument, New Castle, Delaware, USA) to understand the thermal characteristics and degradation behavior. The samples weighed approximately 8.00 mg and were heated from room temperature to 600 ºC at the rate of 10 ºC/min under a nitrogen atmosphere. TGA also helped to understand the PP degradation temperature and to determine the fiber weight fraction of rCF in the rCF-PP composite. The DSC and TGA results helped to determine the processing temperatures for fabricating rCF-PP composite panels via compression molding.

CHAPTER 4- RESULTS AND DISCUSSIONS

4.1 FIBER LENGTH DISTRIBUTION

The initial mean fiber length of rCF used for producing nonwoven mats was 5 mm. Carding is a well-known procedure for fiber alignment, although it results in fiber breakage, as was previously mentioned. Because FLD is directly connected to the mechanical characteristics of composites [83], understanding the effect of manufacturing techniques and processing conditions on FLD is crucial. Since fiber length is preserved in the WL process [84], the FLD was performed only on carded, nonwoven mats. First, the FLD study was performed on carder 1 with a pin length of 1/2" using both the tweezer and ultrasonic methods (Figure 20). The FLD analysis using the tweezer method shows that 301 fibers out of 1572 fall in the range of 3-3.5 mm, i.e., 19% of the fibers are between 3-3.5 mm after carding. The FLD analysis using ultrasonic methods shows that 1288 fibers out of 2500 fall in the range of 0-0.5 mm, i.e., 51.5% of the fibers are in the range of 0-0.5 mm after carding. The mean fiber length (l_m) after carding using the tweezer method was 3.77 mm, whereas with the ultrasonic method it was 0.68 mm. Accordingly, it was found that after carding, l_m was reduced by 24.6% using the tweezer method and by 86.4% using the ultrasonic method.

After the burn-off test, the rrCF obtained were mainly in the form of bundles as seen in Figure 19b. In the tweezer method, one tweezer was used to hold the bundles, while the other tweezer was used to shake the bundles to separate the fibers for the FLD study. Because this process is done by hand and CFs are chosen by hand in a subjective way, as well as the brittle nature of carbon fibers under applied load, this process is susceptible to mistakes. Therefore, the FLD study on carder 2 was carried out with only the ultrasonic method.

Figure 21 shows the FLD analysis via an ultrasonic method on rCF-PP nonwoven mats manufactured on carder 2 with a pin length of 5/8”. Around 1500 fibers were measured, and the FLD data shows that 710 fibers fall in the range of 0.5-1.00 mm i.e., 47.3 % of the fibers are in range of 0.5-1.00 mm after carding. The l_m after carding using

the ultrasonic method was 1.03 mm. Hence, it was observed that there was a 79.4 % reduction in the l_m of rCF after carding on carder 2.

For discontinuous fibers, the critical fiber length (l_c) is one important criterion to understand the load transfer mechanism in the composite. The l_c is the minimum fiber length that must be present to transmit a significant amount of load from the matrix to the fiber before the occurrence of fiber fracture. Equation 5 is used to calculate the critical fiber length [85], [86].

$$l_c = \frac{\sigma_{fu} d_f}{2\tau_i} \tag{5}$$

where σ_{fu} is fiber ultimate tensile strength, d_f is fiber diameter and τ_i is the shear strength of the fiber-matrix interface. Based on the Tresca yield criterion, the value of τ_i can be approximated by assuming that the shear strength of the fiber-matrix interface is the same as the matrix shear strength (Equation 6) [76].

$$\tau_i = \frac{\sigma_m}{2} \tag{6}$$

where σ_m is matrix ultimate tensile strength. The value of σ_m for PP fibers is 23.05 MPa which is obtained via tensile testing as seen in subsequent section. Therefore, using Equation 5, the approximate l_c value is 0.89 mm. The fiber and matrix mechanical properties required to calculate l_c are summarized in Table 0.2. From above, the l_m value for carder 1 is 0.68 mm, whereas for carder 2 the l_m value is 1.03 mm. In carder 1 the $l_m < l_c$, implies that the maximum fiber stress will never reach the maximum fiber strength. In this scenario, the matrix or the fiber-matrix interfacial connection may fail before the fibers reach their ultimate strength. On the contrary, in carder 2 the $l_m > l_c$, which shows that over a large portion of fiber length, the maximum fiber stress may equal the ultimate fiber strength [87]. Hence for further characterization data, carder 2 was used.

Overall, FLD data demonstrates that both carders significantly reduce the l_m of rCF. This is due to the absence of sizing and fiber degradation in

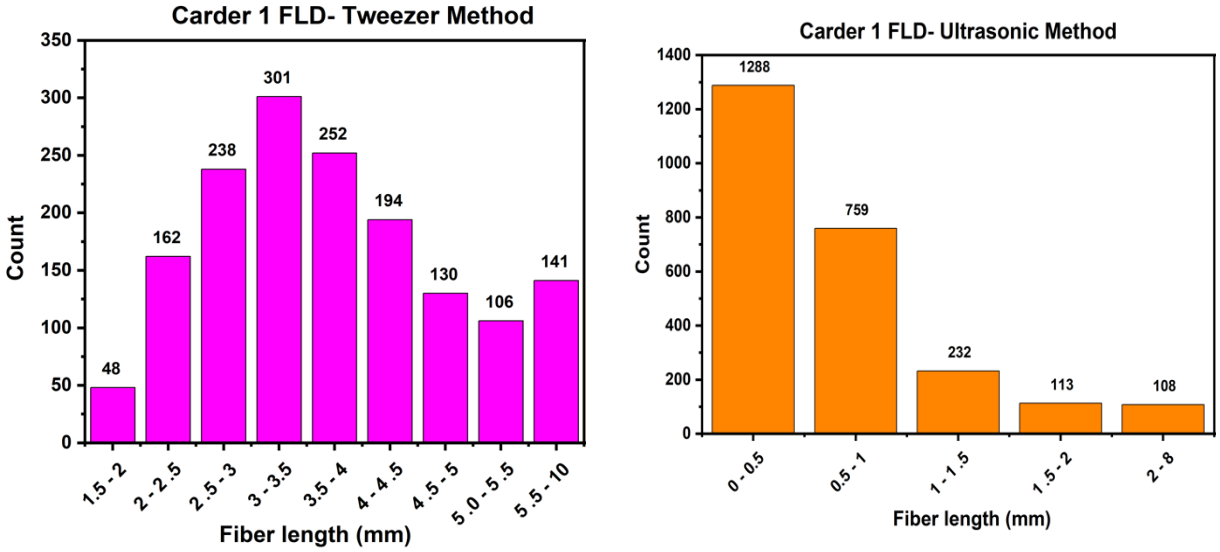


Figure 20: Carder 1- FLD study using both tweezer and ultrasonic method

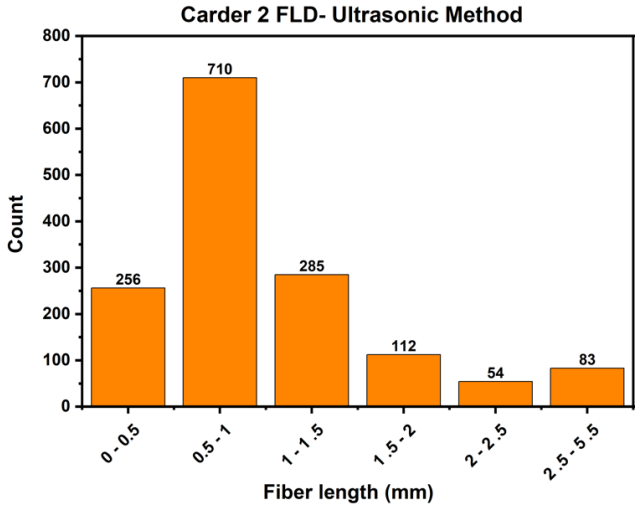


Figure 21: Carder 2- FLD study using ultrasonic method

pyrolysis process. Due to the absence of sizing, the rCF experienced higher friction and stress during carding, which affected the l_m of the fibers. In addition, following the carding process, the nonwoven mat underwent pyrolysis so that the matrix could be removed and rrCF could be obtained for FLD analysis. In this process, the rrCF may have degraded further, increasing the likelihood of fiber breakage. Heilos et al. [10] at the Saxon Textile Research Institute found that lack of sizing on rCF had an effect on fiber-matrix interaction, and that rrCFs degraded during pyrolysis (burn-off) indicated by fracture on fibers.

4.2 FIBERS MIXING TECHNIQUE

To establish a method that deagglomerated and homogeneously mixed the fibers, five different mixing tests were carried out, as shown in Table 0.3. The results of those mixtures are summarized in Table 0.1. Compared to mix tests 1-3, mix tests 4 and 5 showed promising results where rCF and PP fiber mixture appeared to have been deagglomerated and homogeneously mixed. The mix test 1-3 were dry mixes, and the results showed that the rCF-PP mixture kept expanding in the container, and eventually, it stopped mixing beyond a certain point, resulting in an improper fiber mixture. To tackle this issue, water and IPA was introduced as a mixing solvent in mix test 4 and 5, respectively. The results showed that water and IPA solvents prevented the fiber mixture from expanding within the container and aided in achieving a homogeneous rCF-PP fiber mixture.

Further, fibers from five different mixes were fed to a carder 1 to produce five different rCF-PP nonwoven mats. The mats were consolidated into compression molded panels and were tested for the flexural test. The flexural mechanical data is discussed in subsequent section.

4.3 MECHANICAL CHARACTERIZATION

As mentioned in previous sections, carding is a dry-laying mechanical process that aims to disentangle the fibers into individual fibers to generate highly aligned nonwoven preforms. On the contrary, WL is a wet laying process that aims to produce randomly aligned (isotropic) nonwoven preforms. In this section, two methods are compared based

Table 0.1: Results of premixing of rCF-PP using RAM technique

Mixes	Polystyrene vessel size	Observations
	Scoping test (rCF) 16 oz	Increase in volume as time went on
Mix 1	32 oz	1) Fill was extremely high
		2) The mixture expanded further as mix continued
Mix 2	32 oz	Less fibers fill height but still expanded in container
Mix 3	32 oz	Time was increased and the fill was decreased. Fiber's agglomerations still visible
Mix 4	300 ml water 32 oz	The addition of water aided in mixing and fibers appeared to deagglomerate and homogeneously mixed
Mix 5	300 ml IPA 16 oz	The addition of IPA aided in mixing and fibers appeared to deagglomerate and homogeneously mixed

Table 0.2: Characteristics of composite components

Property	Value	Unit
rCF ultimate tensile strength, σ_{fu}	4100[a]	MPa
rCF tensile modulus, E_f	259[a]	GPa
Mean fiber length after carding, l_m	1.03	mm
Critical fiber length, l_c	0.89	mm
rCF fiber diameter, d_f	5	µm
Ultimate PP tensile strength, σ_m	23.05	MPa
PP matrix tensile modulus, E_m	1.24	GPa
Interfacial shear strength, τ_i	11.5	MPa

[a] Obtained from technical data sheet

on their mechanical properties and the variables affecting those properties.

4.3.1 CARDER-1 MECHANICAL PROPERTIES

Initially, the fibers from mix 1-5 were fed into a carder 1 to produce five different rCF-PP nonwoven mats. The mats were molded into panels and were tested for flexural properties. The flexural data for mix tests 1–5 can be seen in Figure 22.

The results showed that the flexural strength and modulus of the composite from mix test 4 showed higher properties than other mixes. This outcome can be attributed to the water used in mix test 4, where the fibers seemed completely deagglomerated and well-mixed. Also, mix test 5 showed a homogeneous fiber mixture with IPA as a mixing solvent. In addition, the mix tests 1-3 and 5 showed similar flexural properties. Hence, the results from RAM mixing test and flexural properties, mix test 4 was selected as the suitable mixing strategy for future study. This decision was made since water would be a more economical alternative as a mixing solvent in than IPA.

In next phase of this study, the rCF-PP mixture was mixed using RAM with water as a mixing solvent. Further, the rCF-PP nonwoven preforms were fabricated using carder 1 and the WL process. The flexural coupons were extracted from the carded panel in the machine direction (MD) and cross-direction (CD). Also, five flexural coupons were extracted from the WL panel. The flexural properties of carded MD, CD, and WL are illustrated in Figure 23. Thereafter, tensile and ILSS specimens were extracted from carded and WL panels. The tensile and ILSS properties of carded and WL rCF-PP composites are shown in Figure 24 and Figure 25 respectively.

The flexural results show that the carded MD composite has higher flexural strength and modulus than the carded CD composite by 36.4% and 27.8%, respectively. Moreover, the flexural strength and modulus of carded MD are 5% and 43% higher than those of WL. The flexural results suggest that carded MD composites exhibit anisotropy when compared to carded CD, while carded MD and WL composites have nearly identical flexural strength.

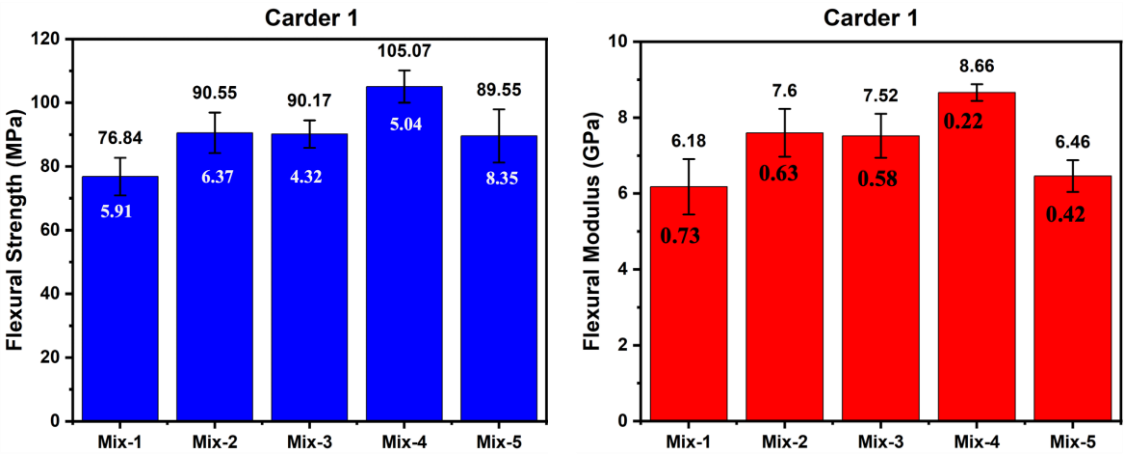


Figure 22: Flexural strength and modulus of rCF-PP composite showing standard deviation manufactured via carder 1 using mix 1-5

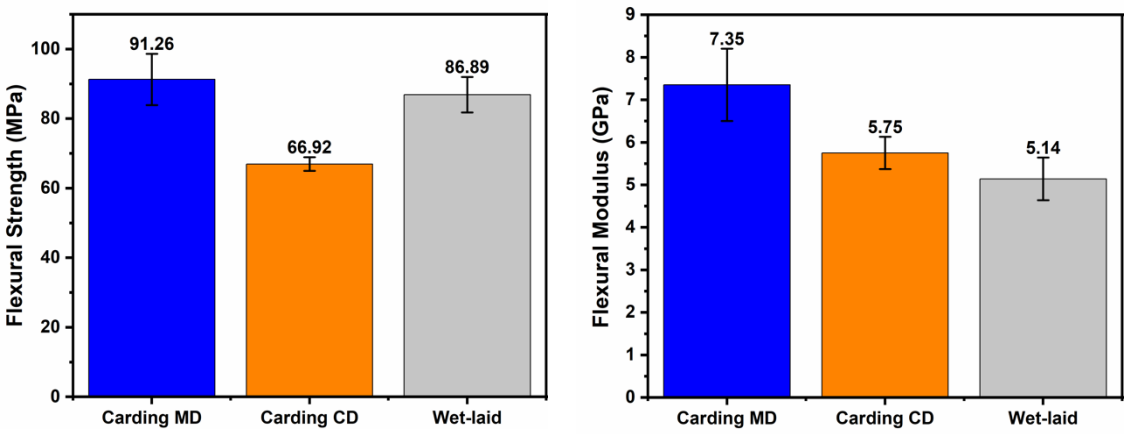


Figure 23: Flexural strength and modulus of rCF-PP carded, and WL composite manufactured via carder 1 with only water as mixing solvent in RAM

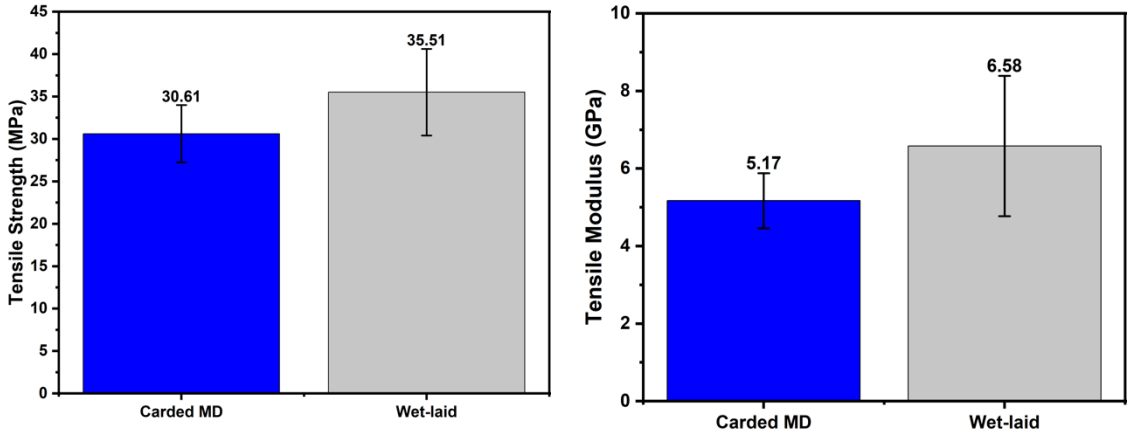


Figure 24: Tensile strength and modulus of rCF-PP carded, and WL composite manufactured via carder 1

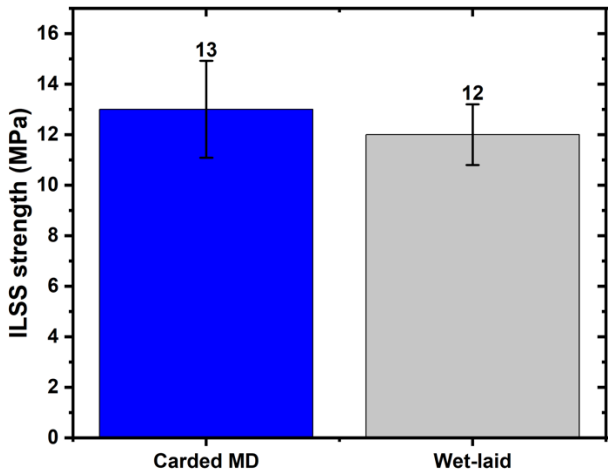


Figure 25: ILSS strength of rCF-PP carded, and WL composite manufactured via carder 1

The tensile data shows that the WL composite has higher tensile strength and modulus than carded MD by 16% and 27.3%. It's possible that the lower tensile strength in the carded MD composite can be attributed to significant fiber breakage that occurred during carding, resulting in a shorter l_m value of rCF post-carding. In contrast, the fiber length was preserved in the WL composite, resulting in a longer fiber length than the critical fiber length.

Further, the ILSS test was run on samples of carded MD and WL composite, with carded MD achieving 13 MPa ILSS strength and WL achieving 12 MPa ILSS strength. The ILSS results show no discernible variation in the properties, and the results comply with the flexural characteristics. According to Thomason et al. [88], fiber length significantly improves polymer composites' mechanical (flexural, tensile, and impact) strength and stiffness. Therefore, l_c plays a crucial role in understanding the mechanical properties of discontinuous fiber-reinforced polymer composites. As mentioned earlier, Equation 5 was used to calculate l_c value of rCF after carding. The obtained l_c was 0.89 mm. Also, from the FLD study the l_m value for rrCF after carding on carder 1 was 0.68 mm. The l_m of rrCF is clearly lower than critical fiber length ($l_m < l_c$). As explained in the FLD section, the fiber may never reach maximum fiber stress, leading to matrix or fiber-matrix interface failure before the fiber reaches its ultimate strength. In addition, handling rCF-PP nonwoven preforms manufactured on carder 1 was quite tricky. After considering all the difficulties and drawbacks associated with the basic drum carder, it was decided to upgrade the carder to a carder 2 for further study.

4.3.2 CARDER-2 MECHANICAL PROPERTIES

Similar procedure as carder 1 was repeated on carder 2 to manufacture rCF-PP nonwoven preform. A burn-off test was performed to recover the rrCF for the FLD study. The results from FLD analysis shows that the l_m value of rrCF was around 1.03 mm. Clearly, in this scenario, $l_m > l_c$. As explained previously, in this case, the fiber may transfer the stress until it reaches ultimate fiber strength over a significant portion of its length. Hence, various mechanical characterization was performed on rCF-PP panels to compare the carding and WL techniques. Based on TGA analysis it was observed that the carded composite showed 27% fiber weight fraction. Also, TGA analysis was not conducted on

WL composite samples as literature suggests no fiber loss during manufacturing [5]. Further, a neat PP panel was fabricated via compression molding and tested to understand the effect of rCF reinforced polymer.

The mechanical properties of rCF-PP composite (carder-2, WL) and neat PP are summarized in Table 0.3. The flexural properties of carded and WL, along with neat PP, are illustrated in Figure 26. The flexural strength of carded MD and carded 0/90 were within 5% of one another; however, compared to WL, the flexural strength of carded MD was 22% higher. Similar trends in flexural strength and modulus were observed. Carding MD and 0/90 flexural moduli were within 10% of each other, but when compared to WL, the carding MD flexural modulus was 72.2%. Overall, the carded flexural properties were higher than WL. The result can be attributed to carded and WL mat thickness variation. The WL mats were well-packed and thinner (~ 3 mm) (Figure 17) compared to carded mats, which were fluffy and thicker (~ 9.5 mm) (Figure 19a). Based on the flexural properties, it can be assumed that carded mats were aligned in MD. Due to carded mats being thicker, the fibers may be oriented differently in various planes, but overall, the fibers will be aligned in MD along the mat thickness. In this way, carded nonwoven mats offer more rigidity while molding than WL, which may explain why the former has superior flexural properties. In addition, the load vs. displacement curves of the aforementioned flexural samples is shown in Figure 27. The slope of the load vs. displacement plot shows the variation in fiber modulus between the carded MD, 0/90, WL, and neat PP samples. The plot clearly shows linear deformation due to ductile failure with a significant difference in elongation behavior between carded and WL samples. In contrast to the significant strain experienced by the fibers in a WL flexural composite, the results show that fibers in carded MD composite successfully transferred stress without significant strain owing to fiber alignment in MD.

Table 0.3:Mechanical properties of carder-2, WL and neat PP samples.

Mechanical Testing			Carding MD	Carding 0/90	WL	Neat PP
Flexural	Strength (MPa)	Mean	105.99	111.21	86.89	43.79
		STD	12.42	8.91	5.1	0.67
	Modulus (GPa)	Mean	8.85	8.07	5.14	1.41
		STD	1.3	0.61	0.5	0.10
Tensile	Strength (MPa)	Mean	62.10	57.20	35.51	23.05
		STD	4.8	1.9	5.1	1.27
	Modulus (GPa)	Mean	13.87	9.20	6.58	1.24
		STD	1.57	2.00	1.81	0.10
ILSS	Strength (MPa)	Mean	15.00	14.00	12.00	—
		STD	0.65	1.16	1.2	—
Izod	Impact energy (KJ/m^2)	Mean	46.30	—	33.66	3.18
		STD	5.88	—	8.05	0.28

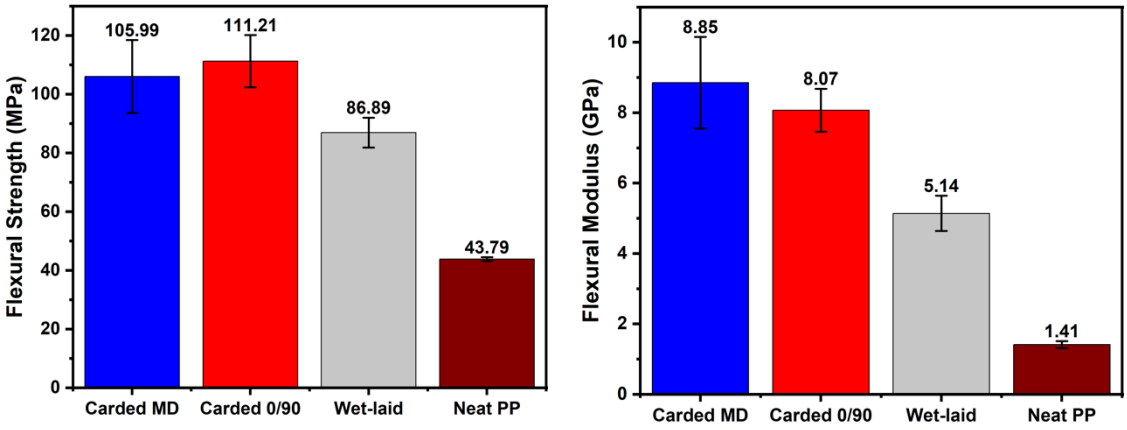


Figure 26: Flexural strength and modulus of rCF-PP carded, and WL composite manufactured using carder 2

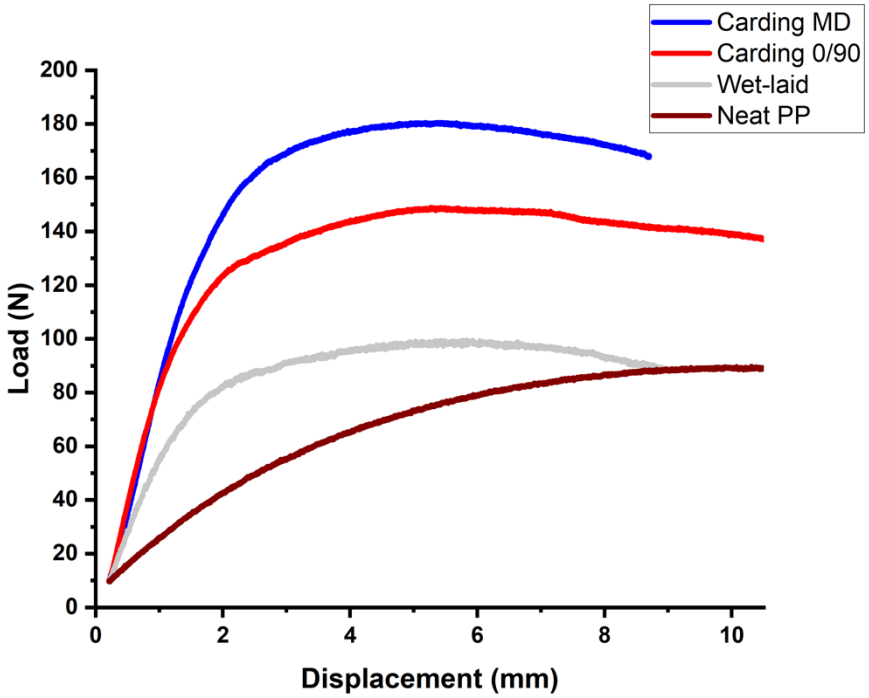
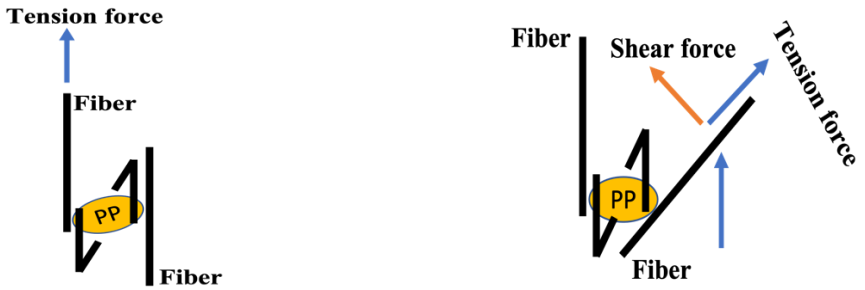


Figure 27: Load vs. displacement curves of carding MD, carding 0/90, wet-laid, and neat PP

Like flexural, tensile test were performed on carded and WL samples. The tensile properties showed similar trend as flexural properties. The nature of the carding process caused the rCF fibers to be oriented in a direction parallel to the carding direction (MD), while the nature of the WL process caused the rCF fibers to be orientated in a random pattern. This phenomenon can be further explained by comparing both processes' tensile properties (Figure 29). As seen in Table 0.3, carding MD and 0/90 tensile strength were within 10% of each other, but when compared to WL (35.51 MPa), the carding MD tensile strength (62.10 MPa) was 75% higher. In addition, the tensile modulus of carded MD was much greater than that of carded 0/90 and WL by 50.8% and 110.8%, respectively. Overall, the carded composite showed significant tensile properties over the WL composite, which can be attributed to the fiber alignment achieved during the carding process. The results of the SEM analysis of fractured tensile composite specimens validates this assumption; see Figure 30 and Figure 31. In the carded MD composite test specimen, most rCF are parallel and aligned with the carding MD, whereas, in the WL composite test specimen, the fibers show random orientation. Also, as seen in the WL test specimen SEM image, there were not many fibers in longitudinal direction contributing to the tensile load, which accounts for the significant gap between tensile properties of carding and WL samples. This highlights the significance of the fiber alignment produced by the carding process. However, SEM analysis of the fractured surface (Figure 32) of the carding composite samples indicated that failure occurred predominantly via fiber pull-out from the PP matrix, showing poor fiber/matrix interfacial bonding, but in the WL (Figure 33) fiber pull out is not apparent due to random fiber orientation but demonstrates weak fiber/matrix bonding. This might be because of non-polar chemical bonds on the surface of the PP matrix, which prevents them from bonding with the rCF's smooth surface [89]. Further, the vast difference in carding and WL tensile properties can be briefly explained by two cases. Case 1: Figure 28a shows that when the fibers are parallel (aligned), most of the force applied to rCFRP is transferred to the fibers, that are stronger than PP. Case 2: On the contrary, Figure 28b shows that when fibers are not parallel (randomly oriented), a portion of the applied



Case-1(a)-Aligned Case-2 (b)-Random

Figure 28: Illustration of force transfer in (a) Aligned composite and (b) Randomly oriented composite

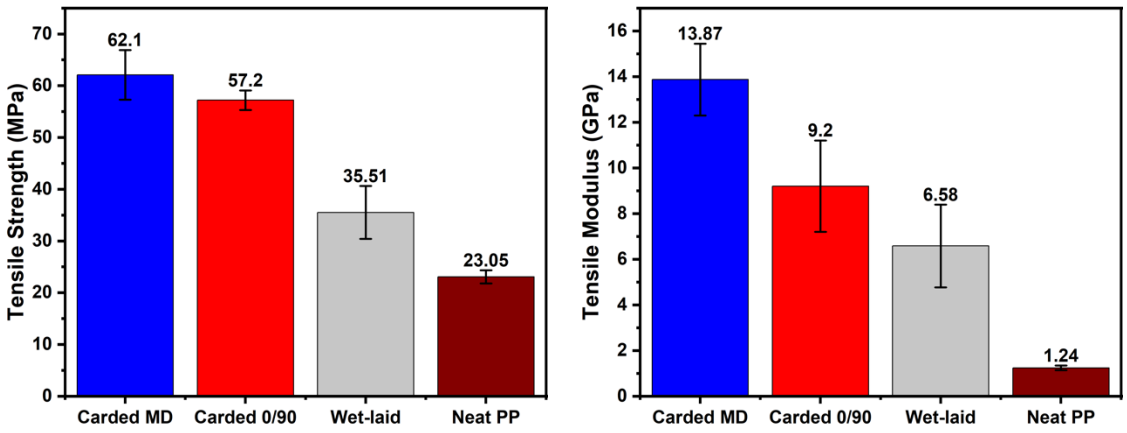


Figure 29: Tensile strength and modulus of rCF-PP carded, and WL composite manufactured using carder 2

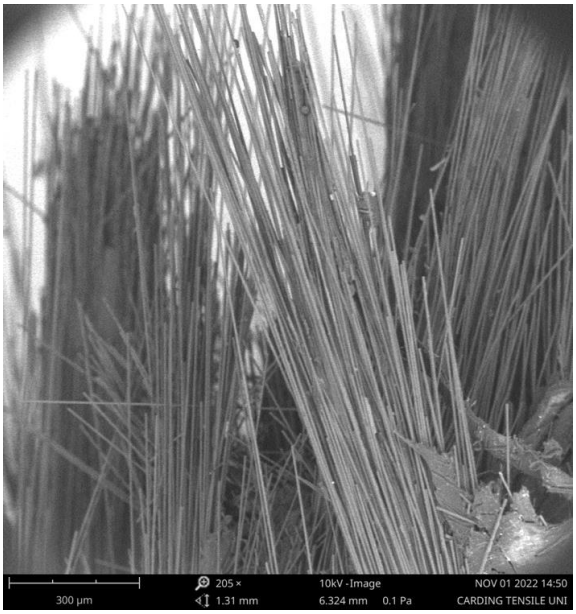


Figure 30: SEM image of carded MD composite tensile test specimen showing fiber alignment.

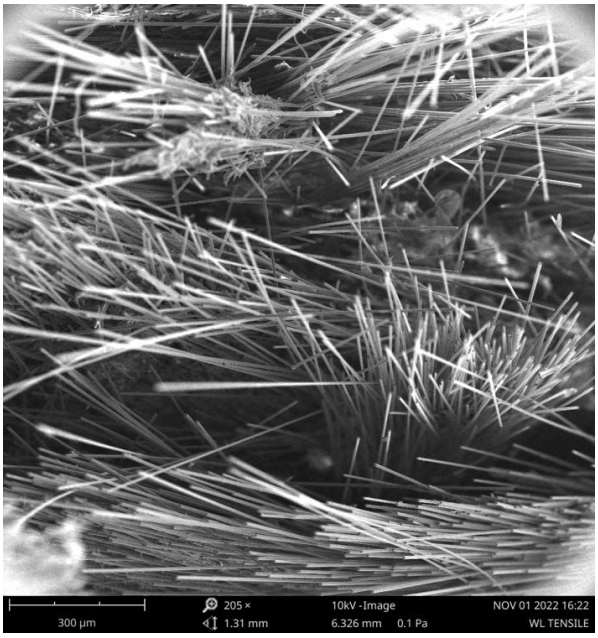


Figure 31: SEM image of WL composite tensile test specimen showing random fiber orientation.

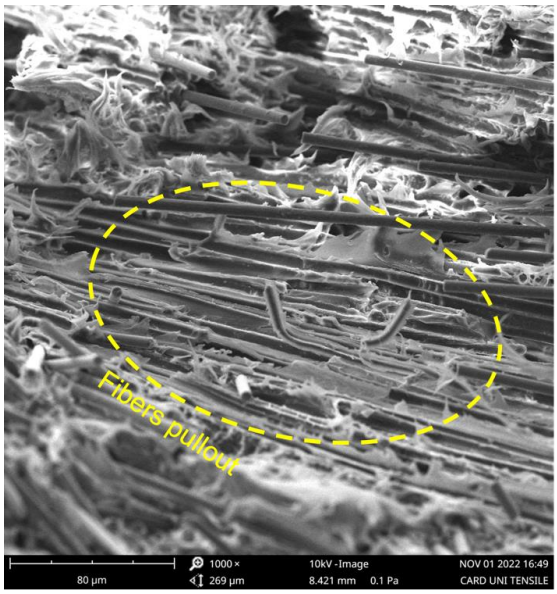


Figure 32: SEM image of carded MD composite tensile test specimen showing fiber pullout

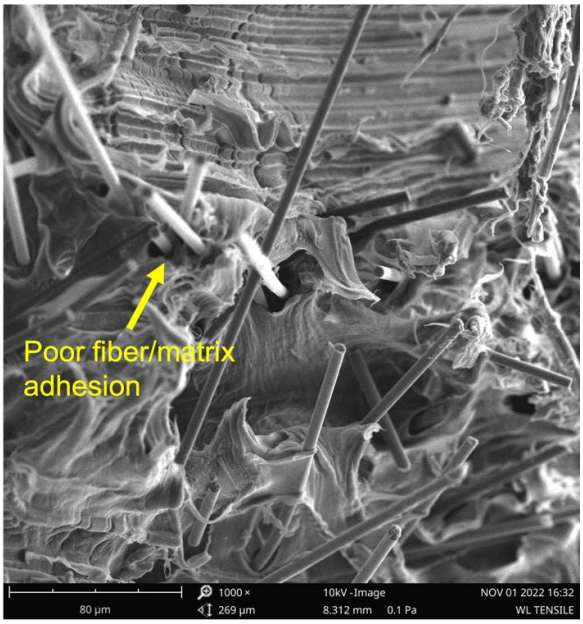


Figure 33: SEM image of WL composite tensile test specimen showing poor fiber/matrix adhesion

force is transferred to the PP as a shear force, leading to the early failure of the rCFRP compared to case 1. Thus, case 1 may be seen in carded composites and case 2 in WL composites. Furthermore, the Ashby plot [5] for rCF composites shows that with the increase of tensile modulus, tensile strength also increases. The literature review shows that most WL composites have low modulus and strength, but carded composites have greater strength at the same stiffness. The difference in properties can be attributed to two critical factors: fiber dispersion and fiber alignment. Generally, highly aligned webs have the best fiber alignment, followed by carding, air-laid, and WL preforms. In addition, the fiber dispersion in WL is often poor due to the absence of a fiber opening stage, as there is in carding [5]. Also, in carding process, premixing rCF-PP using the RAM technique enables greater fiber dispersion during carding, leading to well-dispersed aligned rCF-PP nonwoven preforms as opposed to poorly dispersed randomly oriented WL preforms.

The ILSS test was performed on Carded MD, 0/90, and WL samples to compare the shear strength between the composites plane of lamination. In general, the ILSS properties of carded composites were slightly higher than WL composites. The results show that the ILSS strength of carding MD and 0/90 was within 7% of each other, whereas the ILSS strength of carding MD was 25% higher when compared with WL (Figure 34). As stated previously, the carded rCF-PP nonwoven mats were thicker than WL mats. Consequently, carded mats would have some out-of-plane fiber orientation due to carded pins during carding, which would promote the interlaminar bonding between layers. Hence, carded ILSS properties were higher than WL. The optical images of tested ILSS specimens validate this assumption. Figure 35a shows ILSS tested carded MD composite specimen which did not show any surface failure while ILSS tested WL composite specimen shows interlaminar shear failure in tension Figure 35b.

The Izod test was performed on a carded MD and WL rCF-PP composite to examine how fiber alignment impacts the composite's ability to absorb and distribute energy under impact loading in isotropic and anisotropic composites. The results show that carded MD had an impact energy of 46.30 KJ/m^2 whereas the WL samples reported impact energy of 33.66 KJ/ m^2, i.e., the carded MD composite samples could absorb 37.55% more

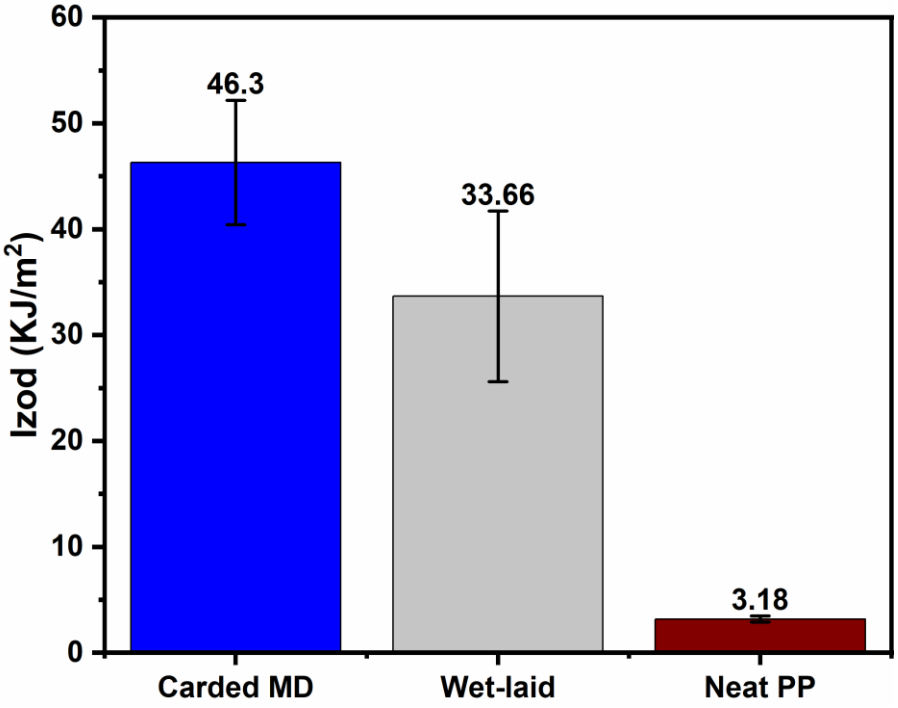
impact energy than WL samples. The results were compared to the neat PP Izod-tested samples (

Figure 36). Two failure modes were observed for carded MD specimens: hinged and complete break. Six of the carded MD specimens failed as hinged while one of them failed completely.

In contrast, the failure mode on WL Izod specimens showed a complete break. The failure modes can be seen in Figure 37 and Figure 38. These results show that fiber alignment in carded MD absorbed more shock by resisting the impact, which led to hinged failure. On the other hand, the random fiber orientation in the WL composite made it less resistant to impact than carded samples and ultimately caused a complete fracture. The analogy of a bundle of sticks can be used to explain this. For instance, if eight of the ten sticks in the bundle are straight, breaking the bundle becomes challenging. However, if only two or three out of ten sticks are straight, breaking the bundle becomes easy and requires much less effort. Think about this phenomenon occurring in aligned carded and WL composites. Suppose the majority of fibers in a carded composite are all oriented in the same direction. In that case, the composite will be more resistant to impact loading and absorb more impact energy than a WL composite, which may only have a few fibers aligned in the same direction.

4.4 THERMAL ANALYSIS

The composite's thermal stability was measured to ascertain the effect of rCF content (30% wt.% fraction) on the thermal degradation of the PP matrix. Figure 39 illustrates the single-step degradation seen in the TGA analysis for both PP and rCF-PP composite. After being heated to 300 °C, both PP and rCF-PP composite showed less than 1% weight loss indicating no moisture content, PP stability, and the composite's maximum permissible processing temperature. There was a significant drop in mass between 380 °C and 480 °C because of the thermal degradation of the material. Due to rCF's greater heat absorption capacity than PP, the degradation temperature of all the composites is higher than that of neat PP [90]. At a temperature of 500 °C, it was observed that the PP had degraded entirely, whereas the composite still had residual mass. It can be seen that the rCF content in 30 wt.% rCF-PP composite was 27%. The 3% loss of rCF content in the composite can be attributed to the escape of rCF bundles

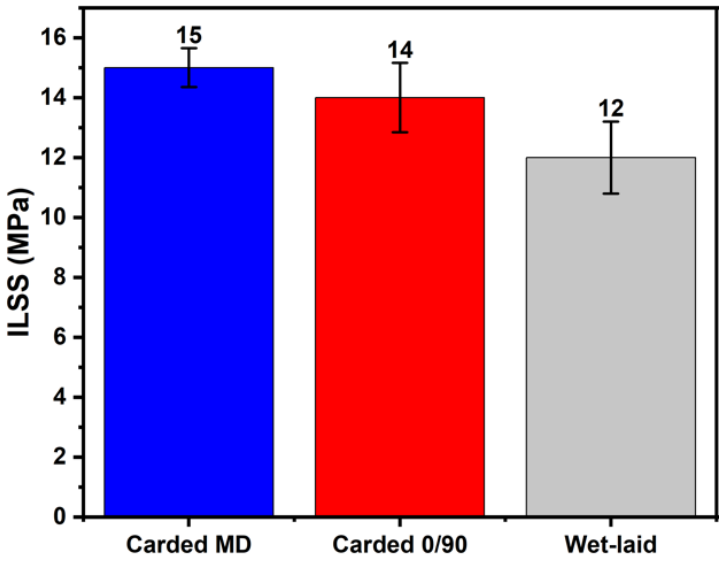
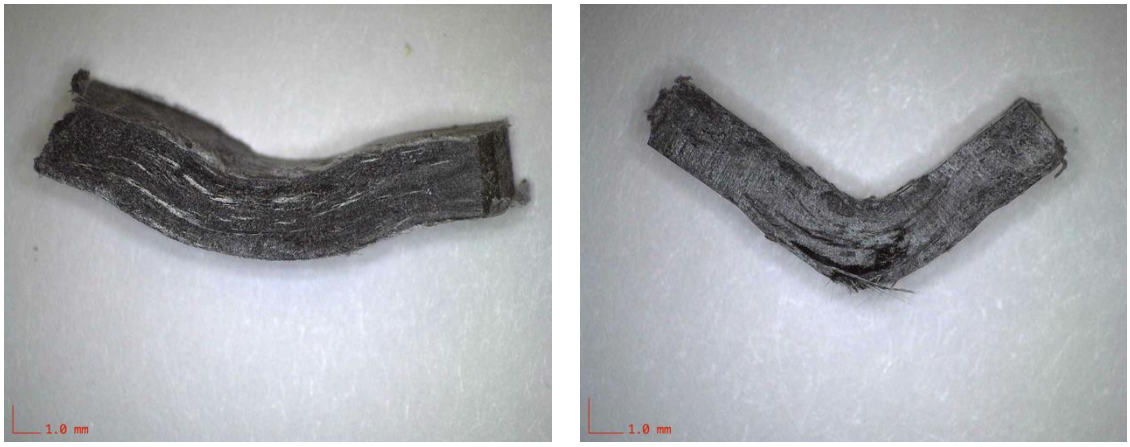


Figure 34: ILSS strength of rCF-PP carded, and WL composite manufactured using carder 2



(a) (b)

Figure 35: (a) Carded MD ILSS test specimen, (b) WL ILSS test specimen

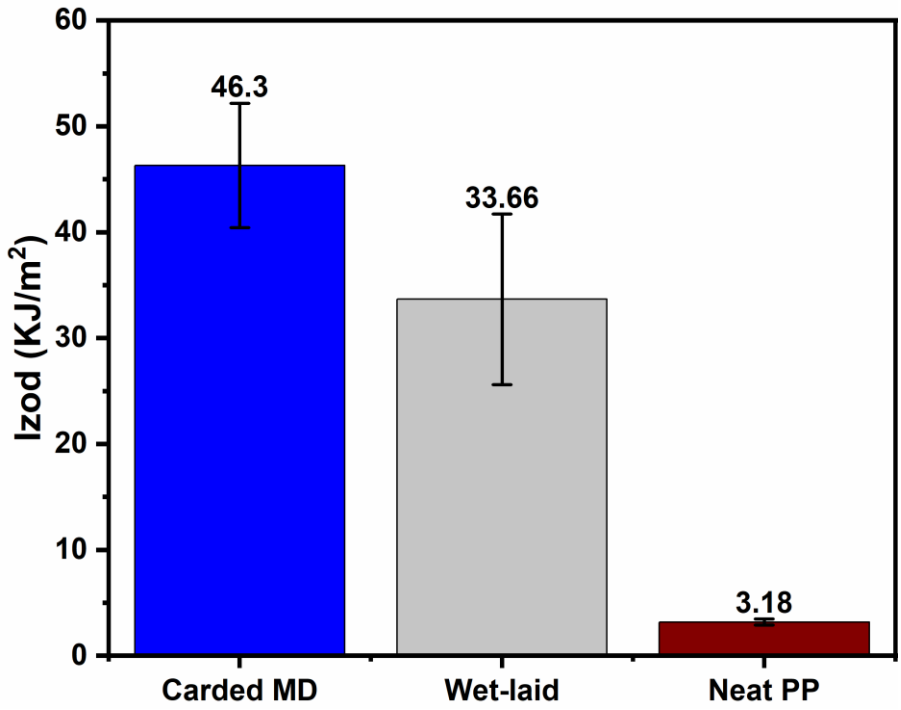


Figure 36: Izod impact break strength of carded and WL rCF-PP composite for notched samples



Figure 37: Carded fractured Izod samples



Figure 38: WL fractured Izod samples

in carding process, as seen in Figure 15d.

Figure 40 and Figure 41 show the DSC results for rCF-PP composite and neat PP, respectively. The melting and crystallization trends were analyzed using the DSC curves. The samples were subjected to heat/cool/heat cycles in the range of 40 ºC to 220 ºC in the presence of nitrogen gas. Peak melting and peak crystallization temperatures of the rCF-PP composite were determined using DSC analysis. The influence of rCF on those temperatures was verified using DSC analysis of neat PP. The first heat cycle was used to eradicate any traces of thermal history on the PP resin. During the cooling cycle, it was observed that PP begins to recrystallize at 114.7 ºC in rCF-PP composite and 111.6 ºC in neat PP. Following the completion of the last heating cycle of the DSC curve, it was observed that the melting point of rCF-PP and neat PP was 163ºC and 162ºC respectively. It was observed that the addition of rCF into PP have clearly no effect on the melting temperature of PP. Equation 4 was used to calculate the degree of crystallinity (X_c). The melting enthalpy (ΔH_m) for rCF-PP (91.22 J/g) and neat PP (114.4 J/g) were obtained from DSC cooling curves. The X_c for rCF-PP composite, and neat PP was calculated to be 43.6% and 54.7% respectively. It is observed that with the addition of 30 wt.% rCF to PP, the crystallinity of PP decreases. Hence, increasing the weight fraction of rCF reduces the overall crystallization of PP. rCF can act as a suitable nucleating agent because it speeds up the nucleation process and reduce the range of crystallite sizes [91]. DSC and TGA results helped to identify the lower (163ºC) and upper (300ºC) temperature limit for processing parameters in this work.

4.5 THEORETICAL APPROACH

The Halpin-Tsai equations [92] are very well known to provide a theoretical framework for predicting the elastic properties of discontinuously aligned fiber composites. According to Mallick [87], the Halpin-Tsai approach is used to determine the longitudinal and transverse characteristics of aligned discontinuous fiber composites, which in turn enables the calculation of the modulus of randomly oriented discontinuous fiber composites. The tensile modulus of aligned fiber composited was calculated by

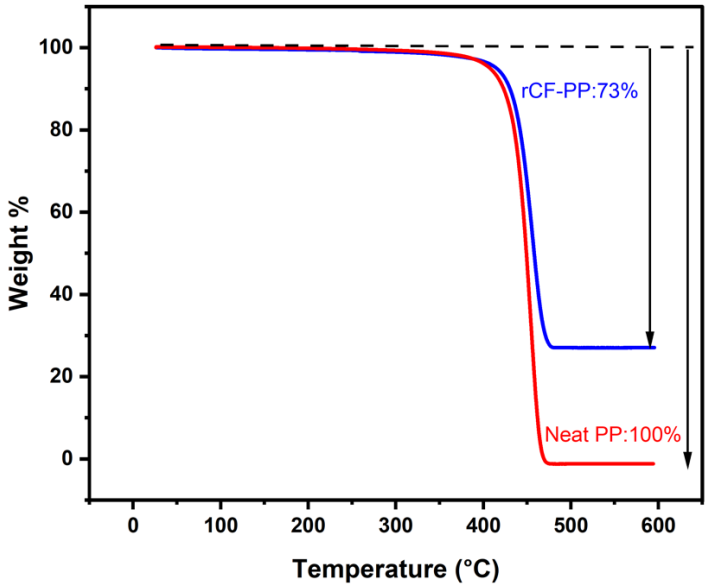


Figure 39: TGA results for neat PP and rCF-PP composite

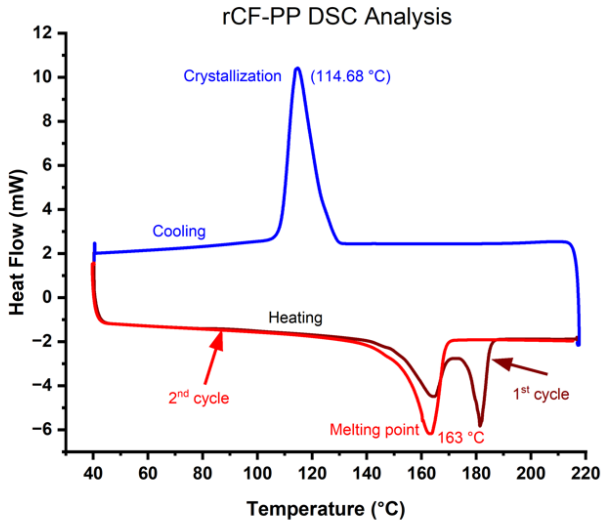


Figure 40: DSC analysis for rCF-PP composite showing heat-cool-heat cycle from room temperature to 220 °C

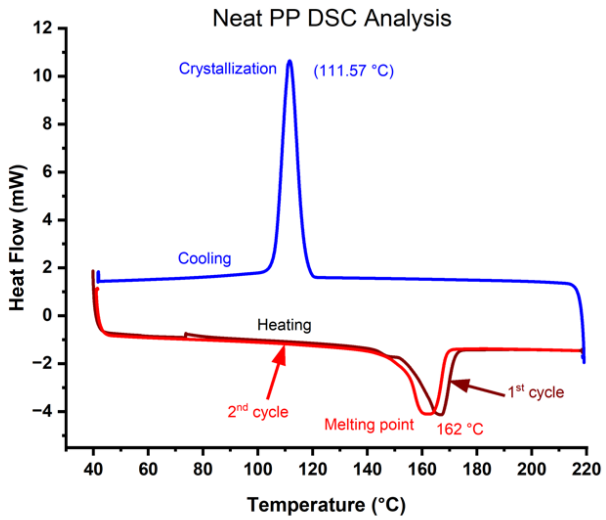


Figure 41: DSC analysis for neat PP showing heat-cool-heat cycle from room temperature to 220 °C

Equations 7 and 8. These equations assume a circular fiber cross-section, perfect bonding between fibers and matrix, fibers arrangement in a square array, a uniform distribution of fibers across the matrix, and the matrix is free of voids. For these assumptions, the longitudinal modulus (E_L) of a discontinuous fiber composite is computed as follows:

$$E_L = \frac{1 + 2\left(\frac{l_m}{d_f}\right)\eta_L \nu_f}{1 - \eta_L \nu_f} E_m \tag{7}$$

and the transverse modulus (E_T) of a discontinuous fiber composite is given by

$$E_T = \frac{1 + 2\eta_T \nu_f}{1 - \eta_T \nu_f} E_m \tag{8}$$

η_L, η_T, and ν_f are computed as follows:

$$\eta_L = \frac{\left(\frac{E_f}{E_m}\right) - 1}{\left(\frac{E_f}{E_m}\right) + 2\left(\frac{l_m}{d_f}\right)} \tag{9}$$

$$\eta_T = \frac{\left(\frac{E_f}{E_m}\right) - 1}{\left(\frac{E_f}{E_m}\right) + 2} \tag{10}$$

$$\nu_f = \frac{w_f/\rho_f}{(w_f/\rho_f) + (w_m/\rho_m)} \tag{11}$$

Where (l_m/d_f) is fiber aspect ratio, ν_f is fiber volume fraction, E_f is fiber modulus, E_m is matrix modulus, w_f is fiber weight fraction, ρ_f is fiber density, w_m is matrix weight fraction, and ρ_m is matrix density.

Further, the tensile modulus of a randomly oriented discontinuous fiber composite (E_{random}) is calculated using Equation 12.

$$E_{random} = \frac{3}{8}E_L + \frac{5}{8}E_T \quad (12)$$

The tensile modulus of the carded MD composite was calculated using Equations 7 and 8, whereas the tensile modulus of the WL composite was estimated using Equation 12. The w_f and w_m values were obtained from the TGA analysis. The rCF w_f was found to be 0.27 g, whereas the w_m was 0.73 g. The rest of the values are summarized in Table 0.1 Table 0.2. The aspect ratio (l_m/d_f) was calculated to be 206 based on the carded fiber length and the rCF diameter. However, when the aspect ratio is more than 100, the l_m or aspect ratio has almost no effect on the elastic modulus of composites [93]. Because of this the suitable critical value of (l_m/d_f) = 100 was used.

The theoretically estimated tensile modulus and experimental values are presented in Table 0.4. The predicted tensile modulus of carded MD and WL composites were much higher than the experimental data (Table 0.4). Manis et al.[8] found that the number of worker-stripper pairings in a carding machine is directly related to the degree of fiber orientation in the nonwoven preform, which is ultimately reflected in the mechanical properties of the composite. This study used a simple two-cylinder tabletop carder without any worker-stripper cylinders. Therefore, only partial fiber alignment would be typical in carded composite with such a basic carder. Additionally, the elastic modulus predicted by Halpin-Tsai equations assumed fully aligned fibers with a uniform FLD. This might be the reason the theoretical elastic modulus was overestimated.

Table 0.4: Comparison of theoretical and experimental results of tensile modulus of carded MD and WL composites.

Tensile modulus	**Carded MD**	**WL**
Theoretical (GPa)	22.46	9.44
Experimental (GPa)	13.87	6.58
Difference (%)	61.93	43.47

CHAPTER 5- CONCLUSIONS

In this study, a unique RAM technique with different mixing strategies was used to homogeneously premix the rCF and PP fibers. Carding and WL processes were used to manufacture discontinuous rCF reinforced PP nonwoven preforms from premix fibers. Two different carding systems were used to evaluate the effect of different carding elements (such as: pin length, cylinder width, combing brush) on nonwoven preforms. Both the processes were compared using fiber length distribution, fiber alignment, mechanical characterization, and microscopic analysis. This study has demonstrated that, the carding process manufactures anisotropic (fibers aligned in machine direction) rCF-PP nonwoven preforms whereas WL process manufactures isotropic (randomly oriented) nonwoven preforms.

The key findings of this study are as follows:

1. It was observed that water was the suitable mixing solvent for premixing fibers in RAM process as water is more economical as well as showed uniform/homogeneous mixing as compared to dry and IPA mixing.
2. The FLD study on rrCF fibers from carder-1 showed that l_m (0.68 mm) < l_c (0.89 mm) whereas carder-2 showed that l_m (1.03 mm) > l_c (0.89 mm). The nonwoven mat removal and handling were quite difficult on carder-1 which led to more fiber breakage. Hence, carder 2 was introduced for further study.
3. The flexural strength of carded MD and carded 0/90 were within 5% of one another; however, compared to WL, the flexural strength of carded MD was 22% higher. Carding MD and 0/90 flexural moduli were within 10% of each other, but when compared to WL, the carding MD flexural modulus was 72.2% higher.
4. The tensile properties showed similar trend as flexural properties. The tensile strength of carding MD and 0/90 were within 10% of each other, but when compared to WL the carding MD tensile strength was 75% higher. In addition, the tensile modulus of carded MD was much greater than that of carded 0/90 and WL by 50.8% and 110.8%, respectively. Overall, the carded composite showed significant tensile properties over the WL composite, which can be attributed to the

fiber alignment achieved during the carding process. The results of the SEM analysis of fractured tensile composite specimens validates this assumption.

5. The ILSS results show that carding MD and 0/90 was within 7% of each other, whereas the ILSS strength of carding MD was 25% higher when compared with WL.
6. The Izod results showed that carded MD had an impact energy of 46.30 KJ/m^2 whereas the WL samples reported impact energy of 33.7 KJ/ m^2, i.e., the carded MD composite samples could absorb 37.5% more impact energy than WL samples. Carded composite's excellent impact energy absorption over WL demonstrated the significance of fiber orientation on the impact properties of discontinuous fiber composites.
7. The tensile properties of carded MD and WL experimental data were compared to discontinuous aligned and discontinuous random theoretical Halpin-Tsai equations respectively. The results showed that theoretical modulus of carded MD was 61.93% higher than experimental whereas theoretical modulus of WL composite was 43.47% higher than experimental.

REFERENCES

[1] Y. Shao et al., “Effect of the Carding Process and Reinforcement Method of Carbon Fiber/Polypropylene Fiber Nonwoven Fabrics on the Anisotropic Mechanical Properties of Hot-Pressed Composites,” Fibers and Polymers, vol. 21, no. 5, pp. 1115–1125, May 2020, doi: 10.1007/s12221-020-9622-4.

[2] S. DORMOHAMMADI, M. REPUPILLI, F. ABDI, Y. I. N. WAN, J. U. N. TAKAHASHI, and H. HUANG, “Multi-Scale Computational Modeling of Short Fiber Reinforced Thermoplastics,” in Proceedings of the American Society for Composites: Thirty-First Technical Conference, 2016.

[3] H. K. Baid, F. Abdi, M. C. Lee, and U. Vaidya, “Chopped fiber composite progressive failure model under service loading,” in SAMPE Conference Proceedings 2015, 2015, pp. 18–21.

[4] N. van de Werken, M. S. Reese, M. R. Taha, and M. Tehrani, “Investigating the effects of fiber surface treatment and alignment on mechanical properties of recycled carbon fiber composites,” Compos Part A Appl Sci Manuf, vol. 119, pp. 38–47, Apr. 2019, doi: 10.1016/j.compositesa.2019.01.012.

[5] P. R. Barnett and H. K. Ghossein, “A Review of Recent Developments in Composites Made of Recycled Carbon Fiber Textiles,” Textiles, vol. 1, no. 3, pp. 433–465, Oct. 2021, doi: 10.3390/textiles1030023.

[6] F. Meng, J. McKechnie, and S. J. Pickering, “An assessment of financial viability of recycled carbon fibre in automotive applications,” Compos Part A Appl Sci Manuf, vol. 109, pp. 207–220, Jun. 2018, doi: 10.1016/J.COMPOSITESA.2018.03.011.

[7] B. Xiao et al., “Characterization and elastic property modeling of discontinuous carbon fiber reinforced thermoplastics prepared by a carding and stretching system using treated carbon fibers,” Compos Part A Appl Sci Manuf, vol. 126, Nov. 2019, doi: 10.1016/j.compositesa.2019.105598.

[8] F. Manis, G. Stegschuster, J. Wölling, and S. Schlichter, “Influences on textile and mechanical properties of recycled carbon fiber nonwovens produced by carding,” Journal of Composites Science, vol. 5, no. 8, Aug. 2021, doi: 10.3390/jcs5080209.

[9] H. Ghossein, A. A. Hassen, V. Paquit, L. J. Love, and U. K. Vaidya, “Innovative Method for Enhancing Carbon Fibers Dispersion in Wet-Laid Nonwovens,” Mater Today Commun, vol. 17, pp. 100–108, Dec. 2018, doi: 10.1016/j.mtcomm.2018.08.001.

[10] K. Heilos, H. Fischer, F. Bremen, M. Hofmann, and A. Miene, “Nonwovens made of Recycled Carbon Fibres (rCF) used for Production of Sophisticated Carbon Fibre-Reinforced Plastics.” [Online]. Available: https://www.researchgate.net/publication/344918870

[11] Brydon A G, “Handbook of nonwovens,” in Handbook of Nonwovens, Russell S J, Ed. Cambridge: Woodhead Publishing Ltd, 2007, pp. 16–546.

[12] F. Kessel et al., “Wet-laid nonwoven based ceramic matrix composites: An innovative and highly adaptable short fiber reinforcement for ceramic hybrid and gradient materials,” J Eur Ceram Soc, vol. 41, no. 7, pp. 4048–4057, Jul. 2021, doi: 10.1016/j.jeurceramsoc.2021.02.040.

[13] H. L. Ma, Z. Jia, K. T. Lau, J. Leng, and D. Hui, “Impact properties of glass fiber/epoxy composites at cryogenic environment,” Compos B Eng, vol. 92, pp. 210–217, May 2016, doi: 10.1016/J.COMPOSITESB.2016.02.013.

[14] Y. Ma, Y. Yang, T. Sugahara, and H. Hamada, “A study on the failure behavior and mechanical properties of unidirectional fiber reinforced thermosetting and thermoplastic composites,” Compos B Eng, vol. 99, pp. 162–172, Aug. 2016, doi: 10.1016/J.COMPOSITESB.2016.06.005.

[15] P. R. Barnett, C. L. Gilbert, and D. Penumadu, “Repurposed/recycled discontinuous carbon fiber organosheet development and composite properties,” Composites Part C: Open Access, vol. 4, Mar. 2021, doi: 10.1016/j.jcomc.2020.100092.

[16] “Corporate Average Fuel Economy (CAFE) | NHTSA.” https://www.nhtsa.gov/laws-regulations/corporate-average-fuel-economy (accessed Aug. 09, 2022).

[17] A. E. Krauklis, C. W. Karl, A. I. Gagani, and J. K. Jørgensen, “Composite material recycling technology—state-of-the-art and sustainable development for the

2020s," Journal of Composites Science, vol. 5, no. 1. MDPI AG, 2021. doi: 10.3390/jcs5010028.

[18] W. J. Joost, "Reducing Vehicle Weight and Improving U.S. Energy Efficiency Using Integrated Computational Materials Engineering", doi: 10.1007/s11837-012-0424-z.

[19] P. K. Mallick, "FIBER-REINFORCED COMPOSITES," 2007.

[20] J. Wölling, M. Schmieg, F. Manis, and K. Drechsler, "Nonwovens from Recycled Carbon Fibres - Comparison of Processing Technologies," in Procedia CIRP, 2017, vol. 66, pp. 271–276. doi: 10.1016/j.procir.2017.03.281.

[21] M. F. Khurshid, M. Hengstermann, M. M. B. Hasan, A. Abdkader, and C. Cherif, "Recent developments in the processing of waste carbon fibre for thermoplastic composites – A review," Journal of Composite Materials, vol. 54, no. 14. SAGE Publications Ltd, pp. 1925–1944, Jun. 01, 2020. doi: 10.1177/0021998319886043.

[22] P. R. Barnett and H. K. Ghossein, "A Review of Recent Developments in Composites Made of Recycled Carbon Fiber Textiles," Textiles, vol. 1, no. 3, pp. 433–465, Oct. 2021, doi: 10.3390/textiles1030023.

[23] "Automotive Composites Market Size 2021-2027 | Global Forecast Report." https://www.gminsights.com/industry-analysis/automotive-composites-market?gclid=EAIaIQobChMI0ID21daV-wIVE73ICh2_wQtZEAMYASAAEgJu8PD_BwE (accessed Nov. 03, 2022).

[24] C. Sealy, "New lease of life for carbon fiber reinforced plastics," Reinforced Plastics, vol. 63, no. 6, pp. 293–295, Nov. 2019, doi: 10.1016/J.REPL.2018.12.067.

[25] "Composites Market Report 2018," 2018.

[26] Pickering SJ and Turner TA, "Research and development in support of carbon fibre recycling," in 2014 The composites and Advanced Materials Expo: CAMX 2014, Orlando, Florida, USA, October 13-16, 2014, Combined Strength, Unsurpassed Innovation, Oct. 2014, pp. 1411–1418.

[27] S. Pimenta and S. T. Pinho, "Recycling carbon fibre reinforced polymers for structural applications: Technology review and market outlook," Waste

Management, vol. 31, no. 2, pp. 378–392, Feb. 2011, doi: 10.1016/J.WASMAN.2010.09.019.

[28] J. Zhang, V. S. Chevali, H. Wang, and C. H. Wang, “Current status of carbon fibre and carbon fibre composites recycling,” Compos B Eng, vol. 193, p. 108053, Jul. 2020, doi: 10.1016/J.COMPOSITESB.2020.108053.

[29] S. J. Pickering, R. M. Kelly, J. R. Kennerley, C. D. Rudd, and N. J. Fenwick, “A fluidised-bed process for the recovery of glass fibres from scrap thermoset composites,” Compos Sci Technol, vol. 60, no. 4, pp. 509–523, Mar. 2000, doi: 10.1016/S0266-3538(99)00154-2.

[30] S. J. Pickering et al., “DEVELOPMENTS IN THE FLUIDISED BED PROCESS FOR FIBRE RECOVERY FROM THERMOSET COMPOSITES.”

[31] J. H. Zhu, P. Y. Chen, M. N. Su, C. Pei, and F. Xing, “Recycling of carbon fibre reinforced plastics by electrically driven heterogeneous catalytic degradation of epoxy resin,” Green Chemistry, vol. 21, no. 7, pp. 1635–1647, 2019, doi: 10.1039/c8gc03672a.

[32] M. Maadandar, “A New Fiber Reinforced Polymer Composite for Infrastructure Applications Using Recycled Carbon Fibers.” [Online]. Available: https://digitalrepository.unm.edu/ce_etds.https://digitalrepository.unm.edu/ce_etds/175

[33] E. Seiler, A. Stark, and J. Forberger, “Recycling von Textilien aus carbonfaserverstärkten Kunststoff-Bauteilen und deren Produktion,” Chemie Ingenieur Technik, vol. 88, no. 4, pp. 500–505, Apr. 2016, doi: 10.1002/cite.201500033.

[34] A. K. Bledzki, H. Seidlitz, K. Goracy, M. Urbaniak, and J. J. Rösch, “Recycling of carbon fiber reinforced composite polymers—review—part 1: Volume of production, recycling technologies, legislative aspects,” Polymers, vol. 13, no. 2. MDPI AG, pp. 1–13, Jan. 02, 2021. doi: 10.3390/polym13020300.

[35] M. Holmes, “Recycled carbon fiber composites become a reality,” Reinforced Plastics, vol. 62, no. 3, pp. 148–153, May 2018, doi: 10.1016/j.repl.2017.11.012.

[36] C. Morin, A. Loppinet-Serani, F. Cansell, and C. Aymonier, “Near Sub-and Supercritical solvolysis of Carbon Fibre Reinforced Polymers (CFRPs) for Recycling Carbon Fibres as a Valuable Resource: State of the Art.”

[37] K. Kooduvalli, J. Unser, S. Ozcan, and U. K. Vaidya, “Embodied Energy in Pyrolysis and Solvolysis Approaches to Recycling for Carbon Fiber-Epoxy Reinforced Composite Waste Streams,” Recycling, vol. 7, no. 1, Feb. 2022, doi: 10.3390/recycling7010006.

[38] J. Zhang, V. S. Chevali, H. Wang, and C. H. Wang, “Current status of carbon fibre and carbon fibre composites recycling,” Composites Part B: Engineering, vol. 193. Elsevier Ltd, Jul. 15, 2020. doi: 10.1016/j.compositesb.2020.108053.

[39] G. Oliveux, L. O. Dandy, and G. A. Leeke, “Current status of recycling of fibre reinforced polymers: Review of technologies, reuse and resulting properties,” Progress in Materials Science, vol. 72. Elsevier Ltd, pp. 61–99, Jul. 01, 2015. doi: 10.1016/j.pmatsci.2015.01.004.

[40] M. Dauguet, O. Mantaux, N. Perry, and Y. F. Zhao, “Recycling of CFRP for High Value Applications: Effect of Sizing Removal and Environmental Analysis of the SuperCritical Fluid Solvolysis,” Procedia CIRP, vol. 29, pp. 734–739, Jan. 2015, doi: 10.1016/J.PROCIR.2015.02.064.

[41] R. Chhabra and V. Shankar, “Liquid Mixing,” in Coulson and Richardson’s Chemical Engineering, Elsevier, 2018, pp. 333–377. doi: 10.1016/b978-0-08-101099-0.00007-0.

[42] “Recycled carbon fiber update: Closing the CFRP lifecycle loop | CompositesWorld.” https://www.compositesworld.com/articles/recycled-carbon-fiber-update-closing-the-cfrp-lifecycle-loop (accessed Nov. 03, 2022).

[43] Uday Vaidya, Advanced Composites – Innovation & experiential learning. composites for students, educators, hobbyists via exciting projects. Knoxville, 2022.

[44] N. Harnby, M. F. Edwards, and A. W. Nienow, Mixing in the Process Industries, Second. London: Reed Educational and Professional Publishing Ltd, 1992.

[45] I. Bauman and I. Bauman, “Solid-Solid Mixing with Static Mixers Taxonomy, Ecology and Utilization of Carob tree (Ceratonia siliqua) and Bay Laurel (Laurus nobilis) in Croatia View project From Grain Byproducts to Functional Food through Innovative Processing (2017-2020) View project Solid-Solid Mixing with Static Mixers,” 2001. [Online]. Available: https://www.researchgate.net/publication/242518205

[46] C. Wightman and F. J. Muzzio, “POWDER TECHNOLOGY Mixing of granular material in a drum mixer undergoing rotational and rocking motions II. Segregating particles,” 1998.

[47] B. N. Reavell, “Practical aspects of liquid mixing and agitation,” Trans Inst Chem Eng, vol. 29, 1951, [Online]. Available: https://www.scopus.com/inward/record.uri?eid=2-s2.0-84869862450&partnerID=40&md5=82e063d7faa37da3899d0a4c13a321c5

[48] L. T. Fan, Y.-M. Chen, and F. S. Lai, “Recent Developments in Solids Mixing,” 1990.

[49] D. Nance, “SIMULATING THE RESONANT ACOUSTIC MIXER,” 2013.

[50] Inc. Resodyn Acoustic Mixers, “ResonantAcoustic ® Mixing.” Accessed: Dec. 19, 2022. [Online]. Available: www.resodynmixers.com Highlight

[51] A. Gillet, O. Mantaux, and G. Cazaurang, “Characterization of composite materials made from discontinuous carbon fibres within the framework of composite recycling,” Compos Part A Appl Sci Manuf, vol. 75, pp. 89–95, Sep. 2015, doi: 10.1016/j.compositesa.2015.05.002.

[52] M. Such, C. Ward, and K. Potter, “Aligned Discontinuous Fibre Composites: A Short History,” Journal of Multifunctional Composites, vol. 2, no. 3, pp. 155–168, 2014, doi: 10.12783/issn.2168-4286/2/3/4/such.

[53] “LabRAM II - Resodyn Acoustic Mixers.” https://resodynmixers.com/product/labram-2/ (accessed Oct. 06, 2022).

[54] “RAM 5 - Resodyn Acoustic Mixers.” https://resodynmixers.com/product/ram-5/ (accessed Oct. 06, 2022).

[55] R. KM and S. L, “Fabrication Techniques of Micro/Nano Fibres based Nonwoven Composites: A Review,” Modern Chemistry & Applications, vol. 05, no. 02, 2017, doi: 10.4172/2329-6798.1000206.

[56] J. Meredith et al., “Recycled carbon fibre for high performance energy absorption,” Compos Sci Technol, vol. 72, no. 6, pp. 688–695, Mar. 2012, doi: 10.1016/j.compscitech.2012.01.017.

[57] S. Pimenta and S. T. Pinho, “The effect of recycling on the mechanical response of carbon fibres and their composites,” Compos Struct, vol. 94, no. 12, pp. 3669–3684, Dec. 2012, doi: 10.1016/j.compstruct.2012.05.024.

[58] P. Feraboli, H. Kawakami, B. Wade, F. Gasco, L. DeOto, and A. Masini, “Recyclability and reutilization of carbon fiber fabric/epoxy composites,” J Compos Mater, vol. 46, no. 12, pp. 1459–1473, Jun. 2012, doi: 10.1177/0021998311420604.

[59] T. Harbers and C. Ebel, “Highly Efficient Production and Characterization of CFRP Made from Recycled Carbon Fibers.” [Online]. Available: https://www.researchgate.net/publication/291342110

[60] Jayachandran Amit, “Fundamentals of Fiber Dispersion in Water,” North Carolina State University, Raleigh.

[61] K. H. Wong, S. J. Pickering, T. A. Turner, and N. A. Warrior, “COMPRESSION MOULDING OF A RECYCLED CARBON FIBRE REINFORCED EPOXY COMPOSITE.”

[62] J. P. Heil, J. B. Gavin, P. E. George, and J. J. Cuomo, “COMPOSITE PANELS MADE FROM THE WETLAY PROCESS USING RECYCLED CARBON FIBER.”

[63] M. Szpieg, M. Wysocki, and L. E. Asp, “Reuse of polymer materials and carbon fibres in novel engineering composite materials,” in Plastics, Rubber and Composites, Dec. 2009, vol. 38, no. 9–10, pp. 419–425. doi: 10.1179/146580109X12540995045688.

[64] K. Giannadakis, M. Szpieg, and J. Varna, “Mechanical Performance of a Recycled Carbon Fibre/PP Composite,” Exp Mech, vol. 51, no. 5, pp. 767–777, Jun. 2011, doi: 10.1007/s11340-010-9369-8.

[65] M. Szpieg, M. Wysocki, and L. E. Asp, “Mechanical performance and modelling of a fully recycled modified CF/PP composite,” J Compos Mater, vol. 46, no. 12, pp. 1503–1517, Jun. 2012, doi: 10.1177/0021998311423860.

[66] H. Wei, T. Akiyama, H. Lee, I. Ohsawa, and J. Takahashi, “MECHANICAL PROPERTIES OF RECYCLED CARBON FIBER REINFORCED THERMOPLASTICS MADE BY CARBON FIBER PAPER,” 2014.

[67] J. Meng, “Study of Carding Dynamics,” 1996.

[68] H. Rong and G. S. Bhat, “Binder fiber distribution and tensile properties of thermally point bonded cotton-based nonwovens,” J Appl Polym Sci, vol. 91, no. 5, pp. 3148–3155, Mar. 2004, doi: 10.1002/app.13470.

[69] Doguc Necmeddin, “Influence of Fiber Types on Fiberweb Properties in High-Speed Carding,” North Carolina State University, Raleigh.

[70] Oscar K. Hsu, “Dry Laid Web Formation,” Sep. 1996.

[71] Datla Vasantha, “The Influence of Fiber properties and Processing conditions on the characteristics of Needled fabrics.,” Raleigh.

[72] J. Meng, A. M. Seyam, and S. K. Batra, “Carding Dynamics Part I: Previous Studies of Fiber Distribution and Movement in Carding Fiber Movement and Distribution on Cards Distribution and movement of fibers on carding el.”

[73] M. M. B. Hasan, S. Nitsche, A. Abdkader, and C. Cherif, “Carbon fibre reinforced thermoplastic composites developed from innovative hybrid yarn structures consisting of staple carbon fibres and polyamide 6 fibres,” Compos Sci Technol, vol. 167, pp. 379–387, Oct. 2018, doi: 10.1016/J.COMPSCITECH.2018.08.030.

[74] “Systems, Devices, And Methods Of Enhancing Carbon Fiber Dispersion In Wet-laid Nonwovens Ghossein; Hicham Kheir ; et al. [University of Tennessee Research Foundation].” https://uspto.report/patent/app/20200080244 (accessed Oct. 12, 2022).

[75] P. Yeole et al., “Characterization of textile-grade carbon fiber polypropylene composites,” Polymers and Polymer Composites, vol. 29, no. 6, pp. 652–659, Jul. 2021, doi: 10.1177/0967391120930109.

[76] N. S. Hmeidat, D. S. Elkins, H. R. Peter, V. Kumar, and B. G. Compton, “Processing and mechanical characterization of short carbon fiber-reinforced epoxy composites for material extrusion additive manufacturing,” Compos B Eng, vol. 223, Oct. 2021, doi: 10.1016/j.compositesb.2021.109122.

[77] Benoit, “Auto measuring fiber length,” Jun. 2016. https://forum.image.sc/t/auto-measuring-fiber-length-1000-measurements/2058/2 (accessed May 04, 2022).

[78] “Designation: D790 − 15′115′1 Standard Test Methods for Flexural Properties of Unreinforced and Reinforced Plastics and Electrical Insulating Materials 1”, doi: 10.1520/D0790-15.

[79] “Standard Test Method for Short-Beam Strength of Polymer Matrix Composite Materials and Their Laminates 1”, doi: 10.1520/D2344_D2344M-13.

[80] “Standard Test Methods for Determining the Izod Pendulum Impact Resistance of Plastics 1 2. Referenced Documents 2.1 ASTM Standards: 2 D618 Practice for Conditioning Plastics for Testing D883 Terminology Relating to Plastics D3641 Practice for Injection Molding Test Specimens of Thermoplastic Molding and Extrusion Materials D4066 Classification System for Nylon Injection and Extrusion Materials (PA) D5947 Test Methods for Physical Dimensions of Solid Plastics Specimens,” 2010, doi: 10.1520/D0256-10.

[81] “Standard Test Method for Tensile Properties of Plastics 1”, doi: 10.1520/D0638-14.

[82] J. Wang et al., “Shear induced fiber orientation, fiber breakage and matrix molecular orientation in long glass fiber reinforced polypropylene composites,” Materials Science and Engineering: A, vol. 528, no. 7–8, pp. 3169–3176, Mar. 2011, doi: 10.1016/J.MSEA.2010.12.081.

[83] K. Balaji Thattaiparthasarathy, S. Pillay, H. Ning, and U. K. Vaidya, “Process simulation, design and manufacturing of a long fiber thermoplastic composite for

mass transit application," Compos Part A Appl Sci Manuf, vol. 39, no. 9, pp. 1512–1521, Sep. 2008, doi: 10.1016/J.COMPOSITESA.2008.05.017.

[84] E. I. du Pont and C. L. T. Iii, "Orientation Behavior of Fibers in Concentrated Suspensions FRANSISCO FOLGAR."

[85] S. Y. Fu and B. Lauke, "Effects of fiber length and fiber orientation distributions on the tensile strength of short-fiber-reinforced polymers," Compos Sci Technol, vol. 56, no. 10, pp. 1179–1190, Jan. 1996, doi: 10.1016/S0266-3538(96)00072-3.

[86] S. Y. Fu, B. Lauke, E. Mäder, C. Y. Yue, and X. Hu, "Tensile properties of short-glass-fiber- and short-carbon-fiber-reinforced polypropylene composites," Compos Part A Appl Sci Manuf, vol. 31, no. 10, pp. 1117–1125, Oct. 2000, doi: 10.1016/S1359-835X(00)00068-3.

[87] "FIBER-REINFORCED COMPOSITES."

[88] J. L. Thomason, "The influence of fibre length and concentration on the properties of glass fibre reinforced polypropylene. 6. The properties of injection moulded long fibre PP at high fibre content," Compos Part A Appl Sci Manuf, vol. 36, no. 7, pp. 995–1003, Jul. 2005, doi: 10.1016/J.COMPOSITESA.2004.11.004.

[89] M. H. Akonda, C. A. Lawrence, and B. M. Weager, "Recycled carbon fibre-reinforced polypropylene thermoplastic composites," Compos Part A Appl Sci Manuf, vol. 43, no. 1, pp. 79–86, Jan. 2012, doi: 10.1016/j.compositesa.2011.09.014.

[90] A. Fernández, M. Santangelo-Muro, J. P. Fernández-Blázquez, C. S. Lopes, and J. M. Molina-Aldareguia, "Processing and properties of long recycled-carbon-fibre reinforced polypropylene," Compos B Eng, vol. 211, Apr. 2021, doi: 10.1016/j.compositesb.2021.108653.

[91] L. Altay et al., "Manufacturing of recycled carbon fiber reinforced polypropylene composites by high speed thermo-kinetic mixing for lightweight applications," Polym Compos, vol. 39, no. 10, pp. 3656–3665, Oct. 2018, doi: 10.1002/pc.24394.

[92] J. C. Halpin, "Stiffness and Expansion Estimates for Oriented Short Fiber Composites."

[93] Fu SY, Lauke B, and Mai YW, Science and engineering of short fibre reinforced polymer composites. Woodhead, 2009.

VITA

Vinit Dilip Chaudhary was born on December 24, 1993. He grew up in Gandhinagar, state of Gujarat, India, until the age of 22. He moved to the United States in 2015 to join his parents in Sweetwater, TN. There Vinit attended Pellissippi State Community College from August 2015-May 2017 for ESL and engineering prerequisite courses. Later, in August 2017, Vinit transferred to the University of Tennessee Knoxville for his undergraduate studies in Mechanical Engineering. As an undergraduate student, he worked under Dr. Uday Vaidya as an undergraduate research assistant at the Fibers and Composites Manufacturing Facility (FCMF) to work on advanced carbon fiber composite materials. Vinit graduated with a Bachelor of Science in Mechanical Engineering in May 2020. As an undergraduate research student, Vinit learned valuable skills and knowledge about composite materials. This led him to pursue a Master of Science degree in Mechanical Engineering at the University of Tennessee Knoxville, where he worked under Dr. Uday Vaidya on recycled carbon fiber composites. During his studies, he traveled to SPE and SAMPE conferences for student poster presentations and won 1st place and 2nd place, respectively. His research focuses on utilizing recycled carbon fiber reinforced thermoplastics via carding process to manufacture nonwoven intermediates and pathways to composites products.